LUND UNIVERSITY

Nanofiltration of kraft black liquor

Process development and techno-economic evaluation

Battestini Vives, Mariona

2024

Document Version:
Publisher's PDF, also known as Version of record

Link to publication

Citation for published version (APA):
Battestini Vives, M. (2024). *Nanofiltration of kraft black liquor: Process development and techno-economic evaluation*. Chemical Engineering, Lund University.

Total number of authors:
1

LUND UNIVERSITY

PO Box 117
221 00 Lund
+46 46-222 00 00

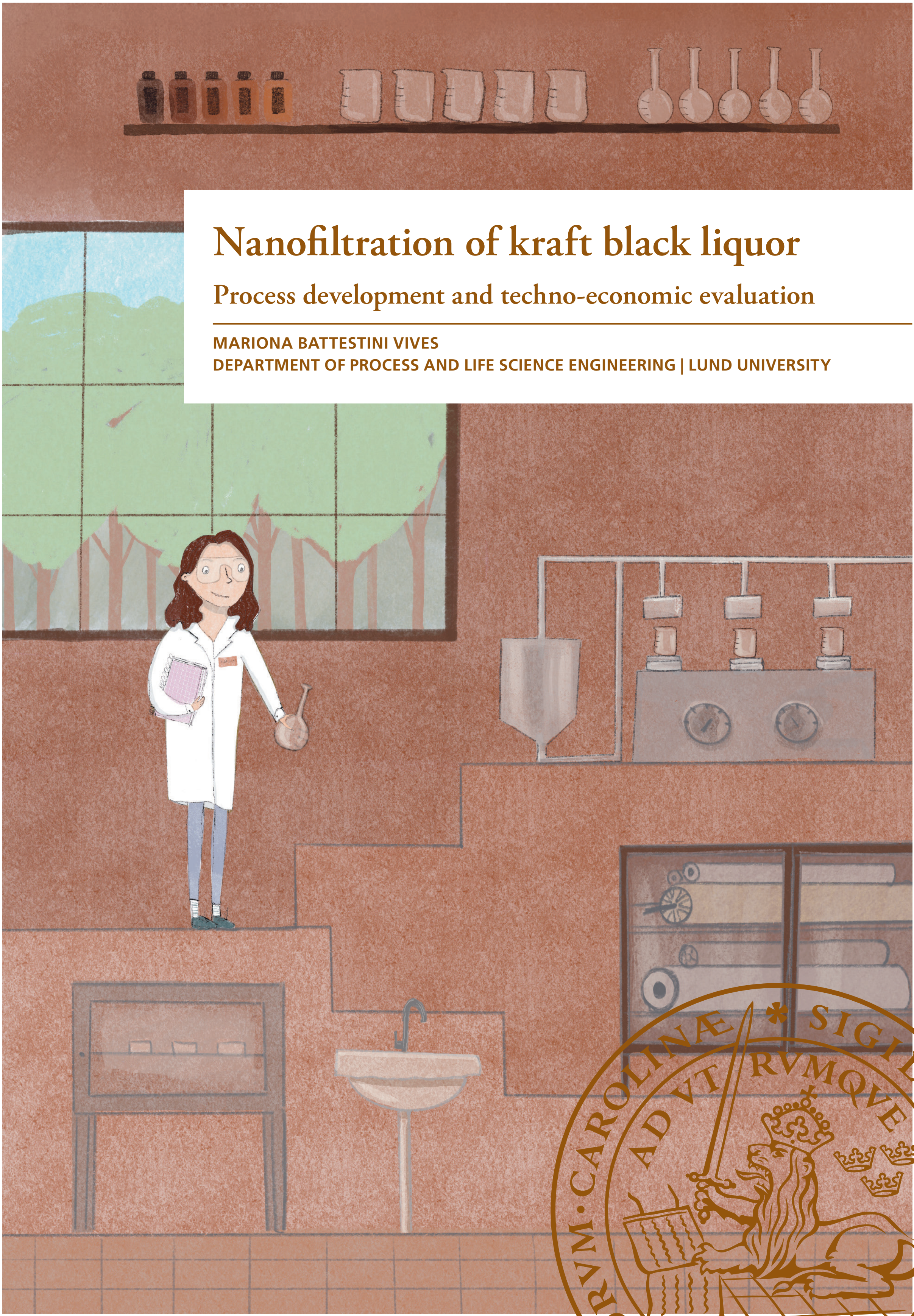

Nanofiltration of kraft black liquor

Process development and techno-economic evaluation

MARIONA BATTESTINI VIVES

DEPARTMENT OF PROCESS AND LIFE SCIENCE ENGINEERING | LUND UNIVERSITY

Nanofiltration of kraft black liquor

Nanofiltration of kraft black liquor

Process development and techno-economic evaluation

Mariona Battestini Vives

DOCTORAL DISSERTATION

Doctoral dissertation for the degree of Doctor of Philosophy (PhD) at the Faculty of Engineering at Lund University, Sweden, to be publicly defended on 25th of October 2024, at 09.00, in Lecture Hall KC:A at the Division of Chemical Engineering

Faculty opponent
Professor Mika Mänttäri
Lappeenranta-Lahti University of Technology School of Engineering Science

Organization: LUND UNIVERSITY

Document name: Doctoral dissertation **Date of issue:** 2024-10-25

Author: Mariona Battestini Vives

Title and subtitle: Nanofiltration of kraft black liquor: Process development and techno-economic evaluation

Abstract: Kraft black liquor (KBL) is a side-stream that is produced during the kraft pulping process, and mainly contains lignin, hemicelluloses, and cooking chemicals, namely sodium hydroxide and sodium sulphide. KBL is usually evaporated and burned in a recovery boiler in order to recover the cooking chemicals and generate energy. However, pulp mills are sometimes limited by the capacity of their recovery boilers. Removing some of the lignin from KBL can decrease the load on the recovery boiler, facilitating an increase in pulp production. Membrane filtration can be used to concentrate lignin from KBL, as it is an energy-efficient separation process that can separate valuable resources from pulping streams based on size or molecular weight.

In this study, an ultrafiltration (UF) permeate obtained by filtering KBL in a membrane filtration pilot plant in a Swedish pulp and paper mill was filtered using nanofiltration (NF). The aim was to investigate how commercial NF membranes perform in concentrating lignin from KBL UF permeate, and at the same time to produce a purified liquor stream that could be reused within the kraft process. This study also focused on optimising the cleaning method for membranes used in the NF of KBL UF permeate, as well as examining the interactions between foulants and the membrane surface. Finally, the techno-economic aspects of implementing such a step in a pulp and paper mill and the costs of cleaning were explored.

Various commercially available NF membranes were used to filter KBL UF permeate. Their performance was assessed in terms of their flux and lignin retention. The membrane selected after this assessment, NF090801, performed well regarding flux and lignin retention, with an average flux of 25 L/(m^2h) and a lignin retention of 94% when operated at 50ºC and 35 bar. At pilot scale, the average flux was 35 L/(m^2h) and lignin retention was 82% when operated at 50ºC and 25 bar. A response surface methodology was then used to optimise the cleaning procedure in order to maximise flux recovery following NF of KBL UF permeate using the NF090801 membrane. The factors studied were temperature, time and cleaning-agent concentration. The investigation found that a flux recovery of 80% can be achieved and the main foulants removed by cleaning for 60 minutes at 40°C with a cleaning-agent concentration of 0.8 wt%. The fouling caused by the filtration of KBL UF permeate using the NF090801 membrane was further studied using in-situ monitoring techniques and surface-characterisation methods. Quartz crystal microbalance with dissipation monitoring indicated that a non-uniform layer of lignin, hemicelluloses, and salts became attached to the membrane surface, and was not fully detached by rinsing with sodium hydroxide. Scanning electron microscopy and energy-dispersive X-ray spectroscopy analysis found that the optimised cleaning method successfully removed the foulants from the membrane surface. Finally, two techno-economic evaluations were performed; these investigated the economic feasibility of implementing a membrane filtration plant within a pulp and paper mill, and whether there are any economic benefits to optimising the cleaning procedure. The techno-economic evaluation showed that implementing a membrane filtration plant with an NF step after a UF step in a pulp and paper mill was economically feasible if the NF permeate was reused during the pulping process, but the lignin was not recovered; and that 16% of current cleaning costs can be saved by optimising the cleaning procedure.

Overall, the findings of this study demonstrate the viability of NF of KBL UF permeate, and the state of readiness of the process to be applied in the pulping industry.

Key words: Nanofiltration, kraft black liquor, lignin, kraft pulping process

Language: English

ISBN: 978-91-8096-062-5

Number of pages: 85

Signature Date 2024-09-12

Nanofiltration of kraft black liquor

Process development and techno-economic evaluation

Mariona Battestini Vives

LUND
UNIVERSITY

Coverphoto by Clara Battestini Vives

Faculty of Engineering
Department of Process and Life Science Engineering
Division of Chemical Engineering

ISBN 978-91-8096-062-5 (print)
ISBN 978-91-8096-063-2 (pdf)

Printed in Sweden by Media-Tryck, Lund University
Lund 2024

Printed matter
3041 0903

Media-Tryck is a Nordic Swan Ecolabel
certified provider of printed material.
Read more about our environmental
work at www.mediatryck.lu.se

MADE IN SWEDEN

To my family.

Table of Contents

Abstract

Kraft black liquor (KBL) is a side-stream that is produced during the kraft pulping process, and mainly contains lignin, hemicelluloses, and cooking chemicals, namely sodium hydroxide and sodium sulphide. KBL is usually evaporated and burned in a recovery boiler in order to recover the cooking chemicals and generate energy. However, pulp mills are sometimes limited by the capacity of their recovery boilers. Removing some of the lignin from KBL can decrease the load on the recovery boiler, facilitating an increase in pulp production. Membrane filtration can be used to concentrate lignin from KBL, as it is an energy-efficient separation process that can separate valuable resources from pulping streams based on size or molecular weight.

In this study, an ultrafiltration (UF) permeate obtained by filtering KBL in a membrane filtration pilot plant in a Swedish pulp and paper mill was filtered using nanofiltration (NF). The aim was to investigate how commercial NF membranes perform in concentrating lignin from KBL UF permeate, and at the same time to produce a purified liquor stream that could be reused within the kraft process. This study also focused on optimising the cleaning method for membranes used in the NF of KBL UF permeate, as well as examining the interactions between foulants and the membrane surface. Finally, the techno-economic aspects of implementing such a step in a pulp and paper mill and the costs of cleaning were explored.

Various commercially available NF membranes were used to filter KBL UF permeate. Their performance was assessed in terms of their flux and lignin retention. The membrane selected after this assessment, NF090801, performed well regarding flux and lignin retention, with an average flux of 25 L/(m^2h) and a lignin retention of 94% when operated at 50ºC and 35 bar. At pilot scale, the average flux was 35 L/(m^2h) and lignin retention was 82% when operated at 50ºC and 25 bar.

A response surface methodology was then used to optimise the cleaning procedure in order to maximise flux recovery following NF of KBL UF permeate using the NF090801 membrane. The factors studied were temperature, time and cleaning-agent concentration. The investigation found that a flux recovery of 80% can be achieved and the main foulants removed by cleaning for 60 minutes at 40°C with a cleaning-agent concentration of 0.8 wt%.

The fouling caused by the filtration of KBL UF permeate using the NF090801 membrane was further studied using *in-situ* monitoring techniques and surface-characterisation methods. Quartz crystal microbalance with dissipation monitoring indicated that a non-uniform layer of lignin, hemicelluloses, and salts became attached to the membrane surface, and was not fully detached by rinsing with sodium hydroxide. Scanning electron microscopy and energy-dispersive X-ray spectroscopy analysis found that the optimised cleaning method successfully removed the foulants from the membrane surface.

Finally, two techno-economic evaluations were performed; these investigated the economic feasibility of implementing a membrane filtration plant within a pulp and paper mill, and whether there are any economic benefits to optimising the cleaning procedure. The techno-economic evaluation showed that implementing a membrane filtration plant with an NF step after a UF step in a pulp and paper mill was economically feasible if the NF permeate was reused during the pulping process, but the lignin was not recovered; and that 16% of current cleaning costs can be saved by optimising the cleaning procedure.

Overall, the findings of this study demonstrate the viability of NF of KBL UF permeate, and the state of readiness of the process to be applied in the pulping industry.

Popular scientific summary

Why do we need to transition to a bio-based economy?

To address the consequences of the climate crisis, we need to transition towards a bio-based economy and utilise biomass resources rather than fossil-based ones. Biorefineries use biomass, such as wood, to produce bio-based products and energy. Researchers are investigating ways to implement biorefinery processes at existing pulp and paper mills to recover valuable compounds from wood that are currently burned or discarded. One way of doing this is by implementing membrane filtration.

How can membrane filtration recover valuable compounds from wood?

Wood is made of cellulose, hemicelluloses and lignin. Lignin binds hemicelluloses and cellulose together in the cell wall of trees and plants. Lignin is currently not fully utilised, and can be used to produce biofuels, bioplastics, resins, and glues. During pulp production, high pressures and temperatures along with chemicals are employed to separate the lignin and hemicelluloses from cellulose in the wood, allowing the cellulose to be transformed into pulp. The remaining wood material is collected in a by-product stream called black liquor, which is typically burned to generate energy. However, lignin could be put to much better use if it were recovered, rather than being burnt.

Lignin can be separated from black liquor using membrane filtration, a common separation process in chemical engineering. A membrane, or dense filter, can separate the components of a solution based on their size. The membrane creates two streams, one with the solution’s larger components retained and another with the smaller components passing through the membrane. In the case of separating lignin, the membrane retains the lignin and other larger components of the black liquor, while allowing water and smaller chemicals, such as salts, to pass through. This process effectively creates two valuable resources: a lignin stream, and a water and salts stream. The lignin stream can be used to make biofuel and bio-based products, and the water and salts stream can be reused within the mill.

What did I do and how does it contribute to the bio-based transition?

In the research presented in this thesis, I explored the possibility of implementing membrane filtration in pulp and paper mills in order to concentrate lignin from black liquor and create a reusable water and salt stream. Different membranes were used to filter black liquor at laboratory scale. Once I identified a membrane that effectively retained the lignin, I conducted pilot-scale tests to further evaluate the membrane’s performance. The results of the pilot-scale experiments were then used to evaluate the economic viability of implementing membrane filtration for lignin recovery in a pulp and paper mill.

To implement membrane filtration effectively, membrane fouling must be studied. Fouling occurs when the membrane becomes clogged, which reduces its capacity and necessitates cleaning. I investigated the parameters of temperature, time, and cleaning-agent concentration that relate to cleaning the membranes used to filter black liquor. Moreover, I identified the specific components in the black liquor that cause fouling, and investigated their interactions with the membrane.

This research provides novel insights and essential knowledge for implementing membrane filtration in pulp and paper mills. While this work represents only a small contribution, I hope that it will add to the collective effort needed to move away from fossil-based resources and transition towards a bio-based economy.

Populärvetenskaplig sammanfattning

Varför behöver vi gå över till ett biobaserat samhälle?

För att förhindra den klimatkris som vi står inför måste vi gå över till en ekonomi, som använder förnybara resurser, till exempel biomassa istället för fossilbaserade resurser. Bioraffinaderier använder biomassa, såsom trä, för att producera biobaserade produkter och energi. Forskare undersöker sätt att implementera bioraffinaderiprocesser vid nuvarande massa- och pappersbruk. Att införliva membranfiltreringssteg i massa- och pappersbruk skulle kunna återvinna värdefulla ämnen från ved, som för närvarande bränns eller kasseras.

Hur kan membranfiltrering återvinna värdefulla föreningar från trä?

Trä är tillverkat av cellulosa, hemicellulosa och lignin. Lignin binder hemicellulosa och cellulosa samman i cellväggen hos träd och växter. Lignin är för närvarande inte fullt utnyttjat och kan användas för att producera biobränslen, bioplaster, hartser och lim. Under massatillverkningen används höga tryck och temperaturer samt kemikalier för att separera ligninet och hemicellulosorna från cellulosa i veden, vilket gör att cellulosan kan utnyttjas för massa. Det återstående trämaterialet samlas i en biproduktström, kallad svartlut, som vanligtvis bränns för att generera energi. Men lignin skulle vara mer värdefullt om det kan återvinnas istället för att brännas.

Lignin kan separeras från svartlut genom membranfiltrering, en vanlig separationsprocess inom kemiteknisk industri. Ett membran, som är ett väldigt tätt filter, kan separera komponenter i en lösning baserat på storlek. Membranet skapar två procesströmmar: en där lösningens större komponenter behålls, och en annan där de mindre komponenterna passerar genom membranet. Vid separering av lignin håller membranet kvar ligninet och andra större komponenter från svartluten, samtidigt som vatten och mindre föreningar kan passera igenom. Denna process skapar effektivt två värdefulla resurser: en ligninström och ett vatten-och-saltström. Ligninströmmen kan användas för att göra biobränslen och biobaserade produkter, och vatten-och saltströmmett kan återanvändas inom massa-och-pappersbruket.

Vad gjorde jag och hur bidrar det till den biobaserade omställningen?

I denna avhandling presenterar jag möjligheten att implementera membranfiltrering i massa- och pappersbruk för att koncentrera lignin från svartlut och skapa en återanvändbar vatten-och-saltström. Olika membran testades i laboratorieskala för att filtrera svartlut. När jag identifierade ett membran som effektivt höll kvar ligninet, genomfördes tester i pilotskala för att ytterligare utvärdera dess prestanda. Resultaten från experiment i pilotskala användes sedan för att utvärdera den ekonomiska lönsamheten av att implementera membranfiltrering för ligninåtervinning i massa- och pappersbruk.

För att implementera membranfiltrering effektivt är det viktigt att studera hur membranet smutsas ned. Nedsmutsning uppstår när membranet blir igensatt, vilket minskar dess kapacitet, vilket kräver rengöring. Jag undersökte de optimala parametrarna - temperatur, tid och rengöringsmedelskoncentration - för rengöring av membranen som används för att filtrera svartlut. Dessutom identifierade jag de specifika komponenterna i svartluten som orsakar nedsmutsningen och deras interaktion med membranet.

Resultaten från denna forskning gav nya insikter och kunskaper som är väsentliga för att implementera membranfiltrering i massa- och pappersbruk. Detta arbete representerar ett bidrag, som kommer att bidra till den kollektiva ansträngning som krävs för att ersätta fossilbaserade resurser.

Resum de ciència popular

Per què hem de fer el pas cap a una bioeconomia?

Per enfrontar-nos a la crisi climàtica actual, hem de canviar el model d'obtenció de recursos necessaris per al funcionament de la societat. El model ideal seria una bioeconomia, en la qual s'utilitza biomassa en lloc de combustibles fòssils com a font d’energia. Les biorefineries són un element clau per fer aquest pas crucial, ja que utilitzen biomassa, com per exemple fusta, per a produir béns i energia. Les plantes papereres són biorefineries, ja que utilizen fusta per a produir paper. La incorporació de mètodes de separació, com ara la filtració per membranes, seria una de les maneres de desenvolupar les plantes papereres i convertir-les en biorefineries més eficaces. Les membranes poden separar components valuosos dels efluents residuals de la indústria paperera que actualment no s'aprofiten, com per exemple, la lignina.

Com es poden separar components valuosos dels efluents residuals de la indústria paperera utilitzant la filtració per membranes?

La lignina és un dels components de les plantes i, per tant, de la fusta, que uneix l'hemicel·lulosa i la cel·lulosa. Durant la producció de paper, es cou la fusta amb productes químics a altes pressions i temperatures per a separar la lignina i l'hemicel·lulosa de la cel·lulosa. La cel·lulosa se separa de la resta de components en forma de pasta, la qual s'utilitza per a fer paper. El material restant de la cocció, que conté la lignina, l'hemicel·lulosa i els productes químics, es recull en un efluent anomenat licor negre. Aquest licor es crema per generar energia. Tanmateix, si se separés la lignina del licor negre, es podria utilitzar per a produir biocombustibles, bioplàstics, resines i coles.

La lignina es pot separar del licor negre mitjançant la filtració per membranes, un procés de separació comú en enginyeria química. Una membrana, o un filtre dens, pot separar components en una solució en funció de la mida. La membrana divideix la solució en dos efluents: un que conté els components més grans de la solució i que la membrana ha retingut, mentre que l'altre conté els components més petits de la solució que han passat a través de la membrana. Quan s'utilitzen membranes per separar la lignina del licor negre, la membrana reté la lignina, alhora que permet que l'aigua i els productes químics més petits, com les sals, passin. Aquest procés de separació crea dos efluents valuosos: un que conté la lignina, que es podria utilitzar per a produir bioproductes i bioenergia, i un altre que conté aigua i sals, el qual es podria reutilitzar a la planta paperera. Mitjançant la implementació de la filtració per membranes per separar la lignina, una planta paperera incrementaria la seva eficacia com a biorefineria, ja que a part de la producció de paper, recuperaria energia i produiria biorecursos.

Com contribueix la meva recerca a desenvolupar la bioeconomia?

En aquesta tesi, he explorat la possibilitat d'implementar la filtració per membranes a la indústria paperera per a separar la lignina del licor negre. Primer, vaig provar diferents tipus de membranes per a filtrar licor negre al laboratori. Un cop vaig identificar una membrana que retenia eficaçment la lignina, vaig fer proves a escala pilot per avaluar-ne el rendiment. Finalment, vaig avaluar la viabilitat econòmica d'implementar la filtració per membranes per a separar la lignina del licor negre a la indústria paperera.

Per implementar la filtració per membranes de manera eficaç, a banda d'avaluar l'eficàcia d'una membrana a l'hora de retenir components, és important estudiar l'embrutament i la neteja de la membrana. L'embrutament es produeix quan la membrana s'obstrueix, la qual cosa en redueix la capacitat i requereix netejar-la. En aquesta tesi, vaig investigar els paràmetres que afecten la neteja de membranes, tal com la temperatura, el temps i la concentració d'agent de neteja. A més, vaig identificar els components específics del licor negre que causaven l'embrutament i com aquests interactuaven amb la membrana.

Aquesta investigació ha proporcionat coneixements essencials per implementar la filtració per membranes a la indústria paperera. Tot i que aquesta tesi representa només una petita contribució, espero que sumi en l'esforç col·lectiu que es necessita per a deixar d'utilitzar recursos fòssils i començar a utilitzar biomassa per a la producció de béns i energia.

List of papers

Paper I

Battestini-Vives M., Thuvander J., Arkell A., Lipnizki F. (2021). Low-Molecular-Weight Lignin Recovery with Nanofiltration in the Kraft Pulping Process. *Membranes*, 12, no 3: 310, https://doi.org/10.3390/membranes12030310

Paper II

Battestini-Vives M., Thuvander J., Arkell A., Lipnizki F. (2024). Pilot-scale nanofiltration and techno-economic evaluation of lignin recovery from kraft black liquor. *[Manuscript submitted for publication]*

Paper III

Battestini-Vives M., Xiao X., Lipnizki F., Rudolph-Schöpping G. (2025). Response surface methodology to optimize membrane cleaning in nanofiltration of kraft black liquor. *Separation and Purification Technology,* 354, 2025, https://doi.org/10.1016/j.seppur.2024.128626

Paper IV

Xiao X., **Battestini-Vives M.**, Lipnizki F., Rudolph-Schöpping G. (2024). Evaluation of the adsorptive behaviour of kraft black liquor on nanofiltration model membranes via quartz crystal microbalance with dissipation monitoring (QCM-D). *[Manuscript]*

Author's contribution to the papers

Paper I

I designed and planned the experiments together with the co-authors. I performed the experiments and the analysis. I evaluated the results with the co-authors. I wrote the paper together with the co-authors.

Paper II

I designed and planned the experiments together with the co-authors. I performed the experiments and the analysis. I evaluated the results. Johan Thuvander performed the techno-economic evaluation. I wrote the paper together with the co-authors.

Paper III

I designed and planned the experiments together with the co-authors. Xiao Xiao and I performed the experiments. The SEM-EDS analysis were done by Daniel Madsen and me. I evaluated the results and performed the techno-economic evaluation. I wrote the paper together with the co-authors.

Paper IV

I designed and planned the experiments together with the co-authors. Xiao Xiao and I performed the experiments and the analysis. Xiao Xiao evaluated the results. Xiao Xiao wrote the paper together with the co-authors.

Acknowledgements

This thesis would not have been possible without the help, support and kindness from the people I have had by my side during my PhD student journey. Therefore, I would like to start by thanking my main supervisor, Prof. Frank Lipnizki, for his trust and support, and for sharing his passion for membranes. I would also like to thank my co-supervisors, Dr Johan Thuvander, Dr Anders Arkell, Dr Omar Abdelaziz and Dr Gregor Rudolph-Schöpping for their great advice on how to navigate being a PhD student, their thorough feedback, and for always having the time to discuss my research.

I would like to thank my colleagues at the Division of Chemical Engineering for a friendly work environment with plenty of fun conversations and long fikas. I would like to thank the membrains of the Membrane Group, for great membrane-related discussions, help with experiments and conference trips. I would especially like to thank Gity and Maria, for helping me navigate the administrative world; Dr Mats Galbe, for his help with computers and lab equipment; and Dr Borbala Erdei, for everything lab related and for her positive attitude.

My biggest thanks go to Miguel, Ximo, and Rubén, for welcoming me into their group, for showing me how everything worked at the department, and for being the best role models.

Many thanks to Xiao, for being a great friend and a fantastic lab partner to work and collaborate with. Many thanks to Medya and Edvin, for being the best friends and colleagues one could have at the division. Many thanks to Selda, Lucy, Joana, Victoria and Ashley, for all the good times in and outside the lab.

Finally, I would like to thank my husband, my family and my friends for all their love, trust and support during the journey.

Abbreviations and symbols

Abbreviations

AFM	Atomic force microscopy
CA	Contact angle
CFV	Cross-flow velocity (m/s)
DoE	Design of experiments
EDS	Energy-dispersive X-ray spectroscopy
KBL	Kraft black liquor
MF	Microfiltration
MWCO	Molecular weight cut-off (Da or kDa)
NF	Nanofiltration
PEG	Polyethylene glycol
PWF	Pure water flux (L/(m^2h))
QCM-D	Quartz crystal microbalance and dissipation
RO	Reverse osmosis
RSM	Response surface methodology
SEM	Scanning electron microscopy
TMP	Transmembrane pressure (bar)
TS	Total solids (g/L)
UF	Ultrafiltration
VR	Volume reduction (%)

Symbols

A_m	Membrane area (m^2)
C	Concentration of cleaning agent (wt%)
C_b	Concentration of solute at the bulk (g/L)
C_m	Concentration of solute at the membrane surface (g/L)
C_p	Concentration of solute at the permeate (g/L)

D	Dissipation (10^{-6})
f	Frequency (Hz)
J	Permeate flux (L/(m^2h))
k	Transfer mass coefficient
NaOH	Sodium hydroxide
P_{feed}	Pressure at the feed side/inlet (bar)
$P_{retentate}$	Pressure at the retentate side/outlet (bar)
$P_{permeate}$	Permeate pressure (bar)
R_{irrev}	Resistance due to irreversible fouling (1/m)
R_m	Hydraulic resistance of the membrane (1/m)
R_{obs}	Observed retention (%)
R_{true}	True retention (%)
R_{rev}	Resistance due to reversible fouling (1/m)
T	Temperature (ºC)
t	Time (minutes)
V_p	Permeate volume (mL or L)
V_0	Initial feed volume (mL or L)
μ	Dynamic viscosity (Pa·s)
$\Delta\Pi$	Difference in osmostic pressure across the membrane (bar)

1. Introduction

Due to the current climate crisis, there is a need to develop and optimise sustainable processes that can assist in minimising global environmental impact [1]. To achieve this, it is essential that society moves away from fossil-based products and energy, and transitions to a bio-based economy.

Improving lignocellulosic biorefineries is an essential step in the transition from a fossil-based economy to a bio-based one [2]. Lignocellulosic biorefineries convert lignocellulosic biomass feedstocks into value-added products, such as biofuels, biopower, biochemicals, and biomaterials [3], and recover valuable components from underutilised process streams [4].

Existing pulp and paper mills are lignocellulosic biorefineries, which use biomass as their feedstock and produce multiple bio-based products (Figure 1). One of the feedstocks used as lignocellulosic biomass in pulp mills is wood, which mainly contains cellulose, hemicelluloses, and lignin. In lignocellulosic biorefineries, such compounds can be separated and purified from the process streams for valorisation using separation processes that have low energy and chemical consumption, high selectivity and efficiency, minimal number of steps, maximum quality of the final product, and easy scalability [5,6]. Membrane filtration has all these characteristics, which makes this separation technology ideal to implement in biorefineries.

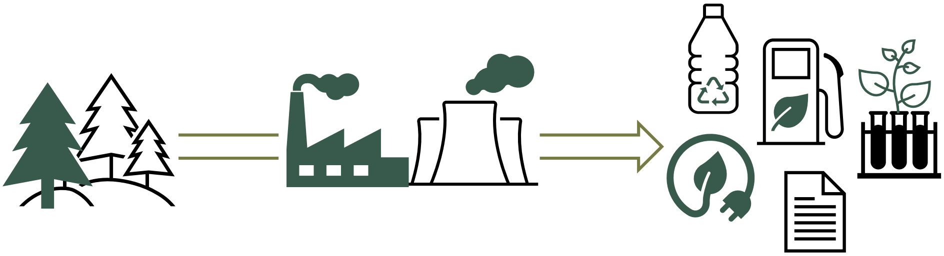

Figure 1: Schematic representation of a lignocellulosic biorefinery that utilises wood as feedstock to generate chemicals, materials, and energy.

1.1. Membrane filtration in lignocellulosic biorefineries

Membrane filtration has several advantages over conventional separation methods, such as evaporation, drying, and filter pressing, including energy-efficiency, high selectivity, operation at moderate temperature, and no need for the addition of chemicals to assist the separation [6]. Membranes are especially advantageous when treating dilute process streams and require minimal space, making them compact and easy to scale up [6].

Pressure-driven membrane processes, such as microfiltration (MF), ultrafiltration (UF), nanofiltration (NF) and reverse osmosis (RO), are very suitable for use in lignocellulosic biorefineries [7]. These processes can be used to dewater and fractionate process streams containing lignocellulosic biomass [6]. Pressure-driven membrane processes have been used in the pulping industry since the late 1960s [8]. At that time, RO and UF were the most common methods of treating bleaching effluents and fractionating spent sulphite liquor. In 1974, a commercial-size plant was installed in Finland by Metsäliiton Teollisuus OY [9]. The plant was for kraft black liquor (KBL) fractionation using UF, and it produced 2000 tons of purified alkali lignin yearly [9]. Since then, membrane processes have been used to treat various process streams at both pilot and industrial scales, facilitating the transition from conventional pulp and paper mills to lignocellulosic biorefineries [8].

The full range of pressure-driven membrane processes has been considered by researchers in the pulp and paper industry in relation to the concentration and fractionation of KBL for the purpose of recovering organic and inorganic compounds. MF has been used to remove the colloidal suspended matter from KBL [10], but it has been found that this process has a 10% lower lignin retention than UF [11]. UF is the most studied process for lignin fractionation [12–15], and it has been demonstrated that high-purity KBL lignin can be obtained [16]. A combination of UF and NF has also been investigated for KBL treatment, for organic acid recovery [17], and for lignin recovery [18–21], and it has been shown that multiple steps are beneficial when multiple fractions or components are to be separated from the KBL. The economic feasibility of a UF step [22] and a UF-NF step [19] during the process of extracting lignin from KBL have been investigated, and these studies concluded that UF can extract lignin for 60 €/t, while NF can extract lignin for 46 €/t. However, a UF pretreatment then NF causes the price of the lignin extraction to increase. Researchers have also considered using NF and RO membranes to filter KBL in order to obtain a water permeate, which can be reused within the mill. For example, reduction of organic content has been achieved by concentrating KBL with RO, allowing the permeate to be reused within the pulp mill [8]. In addition, the economic feasibility of the use of NF membranes for dewatering of KBL has been investigated using a process simulation [23], and it has been found that this results in energy savings, and the NF permeate being possible to reuse in the mill.

Research has also focused on membrane development for KBL filtration. For example, polymeric pH-stable membranes have successfully been tested using a model KBL solution, and provided an organic-content rejection of 92% [24]. Polyethersulphone-supported graphene oxide membranes developed in a laboratory have been shown to operate under high pH and moderately high temperatures when filtering KBL, while having up to 98% lignin rejection [25,26]. Another membrane development is laboratory-made mixed matrix NF membranes with activated carbon nanoparticles for treating KBL UF permeate that have a maximum lignin retention of 82% [18]. While all of these membrane developments are promising, significant research efforts are required to scale-up their production to test them on pilot or industrial scale.

While most of the research discussed above has been successful in terms of KBL concentration and lignin separation at laboratory scale, implementing membrane processes in the pulp and paper industry (at industrial scale) poses significant challenges. The cost of separation processes within a biorefinery accounts for a large fraction of the total capital and operating costs [27]. Moreover, membrane fouling decreases the flux and separation performance of the membrane, increasing operational and maintenance costs [28]. Minimising these and achieving an effective and selective process is essential for the implementation of membrane processes, which in turn requires extensive research and development.

1.2. Aim and outline of this thesis

The main aim of this thesis was to investigate the possible implementation of an NF step in an integrated, two-step, pressure-driven UF-NF membrane process in a pulp and paper mill. The NF step involved treating KBL UF permeate in order to concentrate lignin in the retentate, and obtain a permeate that could be reused in the mill. To implement this, several aspects of the process were investigated: finding the ideal membrane for the process at laboratory and pilot scales, optimising the cleaning method, and identifying the foulants that hinder flux recovery. Therefore, the main aim was divided into the following objectives:

(1) Evaluate commercial NF membranes for filtration of KBL UF permeate based on lignin retention and flux at laboratory scale.

(2) Scale up the NF step from laboratory to pilot scale, and evaluate the feasibility of using the NF retentate and the NF permeate in a pulp mill.

(3) Optimise the cleaning method for NF filtration of KBL UF permeate, and quantify the possible savings of implementing the optimised cleaning procedure at industrial scale.

(4) Study the interaction between the foulants and the membrane surface for KBL UF permeate filtration.

Thus, the content of this thesis is based on four interconnected studies (Figure 2) that investigated and reported on the objectives stated above.

In the first study (**Paper I**), a membrane screening was performed at laboratory scale. KBL UF permeate was filtrated using several commercial NF membranes, and they were evaluated based on their permeate flux and lignin retention.

The second study (**Paper II**) used the best-performing membrane of the first study to concentrate lignin from KBL UF permeate at pilot scale in a pulp mill under two different operating conditions. In addition, the NF process was techno-economically evaluated in order to assess the feasibility of concentrating lignin using membrane filtration, as was the use of the NF retentate and NF permeate in the mill.

The third study (**Paper III**) optimised the cleaning procedure using response surface methodology. The goal was to develop a model that could predict flux recovery based on time, temperature, and the cleaning-agent concentration used for the cleaning method. The costs of applying a standard and optimised cleaning method at industrial scale were techno-economically evaluated.

The fourth study (**Paper IV**) investigated how the main organic foulants found in KBL UF permeate, such as lignin and hemicelluloses, interacted with a model membrane surface by using quartz crystal microbalance with dissipation monitoring.

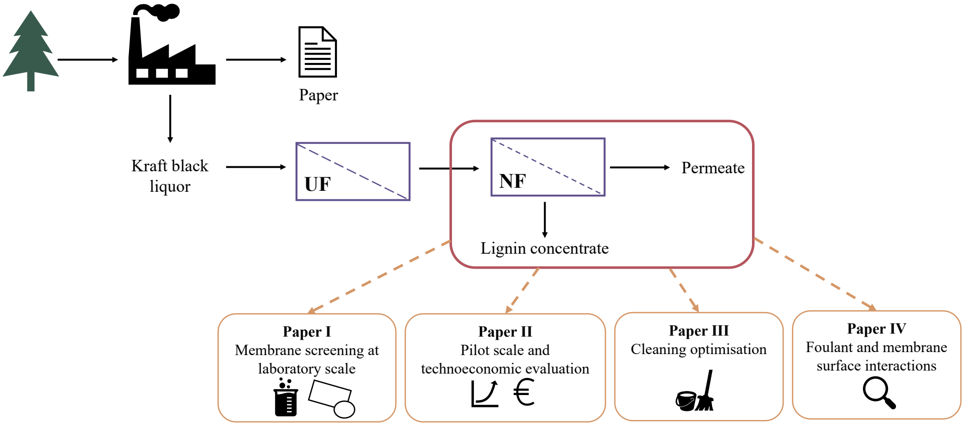

Figure 2: Overview of the process investigated, and the four papers included in this thesis.

2. Background

This chapter introduces the fundamental principles, theories, and methods on which the research reported in this thesis was based. These are linked to the four studies presented in Section 1.2. where relevant.

The chapter starts by introducing pressure-driven membrane filtration, the flux models, and how membrane filtration equipment is usually operated. Membrane fouling is then explained, and the different methodologies used to characterise and monitor fouling are described. In addition, the basics of membrane cleaning and the methods for optimising the cleaning process are explained. The chapter finishes with a brief account of lignin, and the kraft pulping process. Separation of lignin from KBL, which is a process stream that is produced during the kraft pulping process, was one of the main objectives of this work. Therefore, it is important to understand how KBL is produced, and why and how lignin can be separated from this stream.

2.1. Membrane filtration

Membrane filtration is a method of separating the particles of liquids or gases. A membrane is defined as a semi-permeable barrier that is used to separate components based on differences in size or molecular weight, or electrostatic characteristics [29]. The driving force behind this separation is the difference in pressure, concentration, electrical potential, or temperature between the two sides of the membrane [30].

2.1.1. Pressure-driven membrane filtration

The most common type of membrane processes are pressure-driven ones: MF, UF, NF, and RO (Table 1). In these processes, an external pressure is applied in order to separate the feed solution into a permeate and a retentate. Such processes can be classified according to the pore size or molecular weight cut-off (MWCO) of the membrane [31]. MWCO is defined as the weight of a solute that has a rejection of 90% [32]. Usually, the applied pressure increases with decreasing MWCO or denser membranes, but RO, when there is no osmotic pressure, may operate at pressures of 15 bar or less [31].

Table 1: Overview of the operating pressures, characteristics and applications of pressure-driven membrane processes.

	Operating pressure	Pore size/MWCO	Typical application
MF	1 – 2 bar	0.1 – 1 µm	Sterilisation, clarification
UF	1 – 10 bar	1 – 200 kDa	Separation of micromolecular solutes
NF	5 – 40 bar	300 – 1000 Da	Separation of salts and small organic solutes
RO	15 – 150 bar	< 200 Da	Separation of salts and nanosolutes

Pressure-driven membrane processes can be operated in two modes: dead-end or cross-flow (Figure 3) [29]. Dead-end filtration can be compared to coffee filtration: the feed flow (hot water) is perpendicular to the membrane surface (coffee filter). The filtrate created (the coffee), called the permeate, passes through the membrane. The particles retained by the membrane slowly accumulate on its surface, creating a cake layer which increases in thickness over time, causing the filtration performance to in turn change over time. In cross-flow filtration, the feed flow is parallel to the membrane surface, creating shear forces that reduce the accumulation of particles on the membrane surface. During cross-flow filtration, the feed is divided into the permeate and the retentate, where the retentate is the concentrate stream that contains the solutes rejected by the membrane [30].

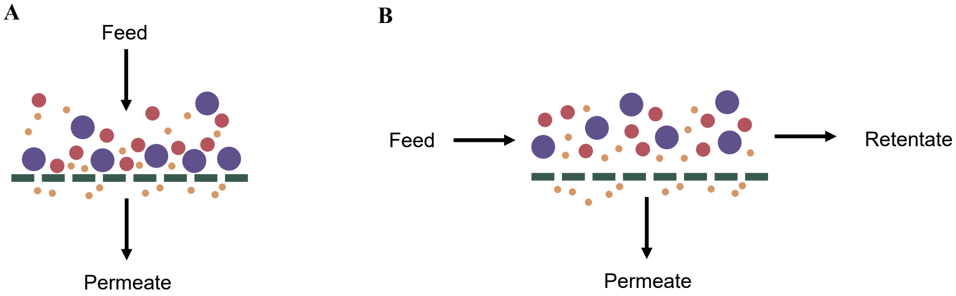

Figure 3: Modes of operation in membrane filtration: (A) dead-end and (B) cross-flow.

The transmembrane pressure (TMP) is the driving force in pressure-driven membrane filtration, and is the difference in pressure between the feed and the permeate [33]. It can be calculated as the average of the pressure between the feed side, P_{feed}, and the retentate side, $P_{retentate}$, minus the pressure on the permeate side $P_{permeate}$ (Equation 1):

$$TMP = \frac{P_{feed} + P_{retentate}}{2} - P_{permeate} \tag{1}$$

2.1.2. Flux models and concentration polarisation

The filtration capacity of a membrane is measured as the flux, J, which can be defined as the volumetric flow of permeate per unit area of the membrane. It is typically expressed as litres per square metre of membrane surface per hour ($L/(m^2h)$). Darcy's law states that the flux is directly proportional to the applied pressure difference, or TMP, and indirectly proportional to the dynamic viscosity of the solvent, μ [34]. If the solvent is pure, the only resistance in the system is the hydraulic resistance of the membrane, R_m. Therefore, the flux can be defined as follows (Equation 2):

$$J = \frac{TMP}{\mu \cdot R_m} \tag{2}$$

If the solvent is only pure water, the flux is defined as the pure water flux (PWF). This flux is used to characterise the membrane resistance and to measure the degree of fouling of the membrane, which will be further described in Section 2.2.1.

If a solution containing one or more solutes is used, rather than a pure solvent, a concentration gradient occurs at the membrane as part of a phenomenon called concentration polarisation. Here, the concentration at the membrane surface, C_m, is usually much higher than in the bulk solution, C_b [35]. The concentration at the membrane surface is determined by the ratio of the convective transport of dissolved material to the membrane, the transport through the membrane, and the diffusion of material back to the bulk stream [35]. The mass transport in the boundary layer can be described by Equation 3:

$$J = k \cdot ln\left(\frac{C_m - C_p}{C_b - C_p}\right) \tag{3}$$

where C_p is the concentration at the permeate and k is the transfer mass coefficient, which describes the diffusion of solutes from the boundary layer into the bulk phase.

When filtering a solution containing one or more solutes, the difference in osmotic pressure, $\Delta\Pi$, across the membrane needs to be considered as it reduces the driving force (Equation 4). The difference in osmotic pressure is the chemical potential that arises due to the difference between the concentration at the feed and the permeate side of the membrane [35]:

$$J = \frac{TMP - \Delta\Pi}{\mu \cdot R_m} \tag{4}$$

There are two important flux definitions in membrane filtration: limiting flux and critical flux (Figure 4). For the filtration of a pure solvent, such as water, the flux increases linearly as the TMP increases. If the solvent contains one or more solutes, the flux will reach a maximum at a certain TMP, then stop increasing. This maximum and pressure-independent flux is called limiting flux [36,37], and is reached due to much of the dissolved material being transported at the membrane surface, causing concentration polarisation and/or fouling. When the flux reaches the limiting flux point, it cannot be increased by just increasing the TMP. However, it can be increased by increasing the temperature or shear forces. The critical flux has been defined in two ways. The strong form of critical flux states that the critical flux is the point at which the flux begins to deviate from the PWF [38,39]. The weak form of critical flux is the point at which the flux deviates from a linear relationship between TMP and flux, that means, if there is immediate adsorptive fouling [38,39].

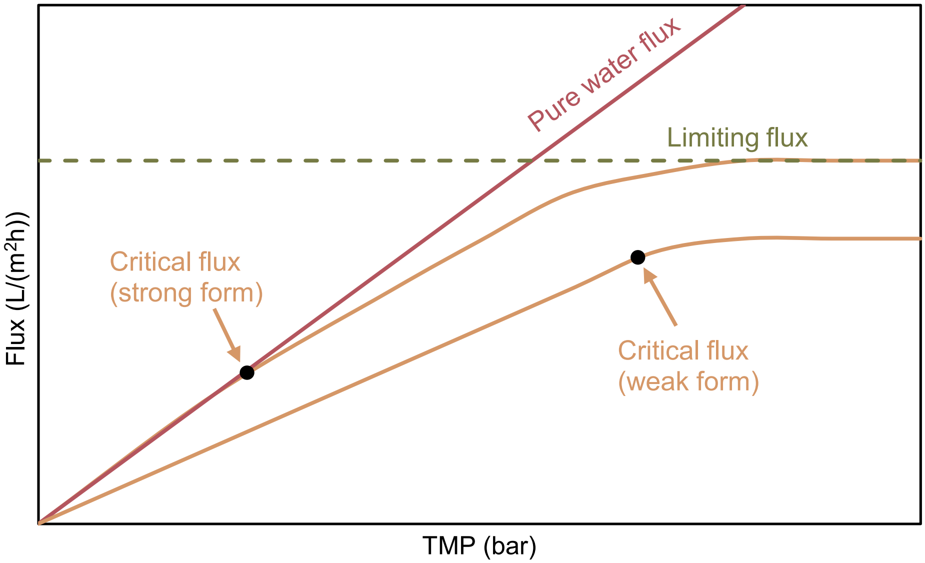

Figure 4: Flux curves showing limiting flux and critical flux.

2.1.3. Membrane filtration equipment operation

Parametric studies are used to determine the optimal operating conditions for membrane filtration systems, in terms of which operating parameters work best with the feed and the membrane. This involves both retentate and permeate being recirculated back to the feed tank (Figure 5A), while operating parameters such as TMP and cross-flow velocity (CFV) are gradually changed. During this process, the retention of the compound or compounds of interest and the permeate fluxes are monitored.

Concentration studies are often used to determine the concentration capacity of the membrane, and to study the retention over time under certain operating conditions.

Here the retentate is recirculated back to the feed tank, while the permeate is constantly withdrawn (Figure 5B). Concentration studies can be operated in a constant-pressure mode, where the TMP is kept constant and the flux naturally decreases as the feed is concentrated; or in a constant-flux mode, where the flux is kept at the desired value and the TMP increases over time in order to maintain that value.

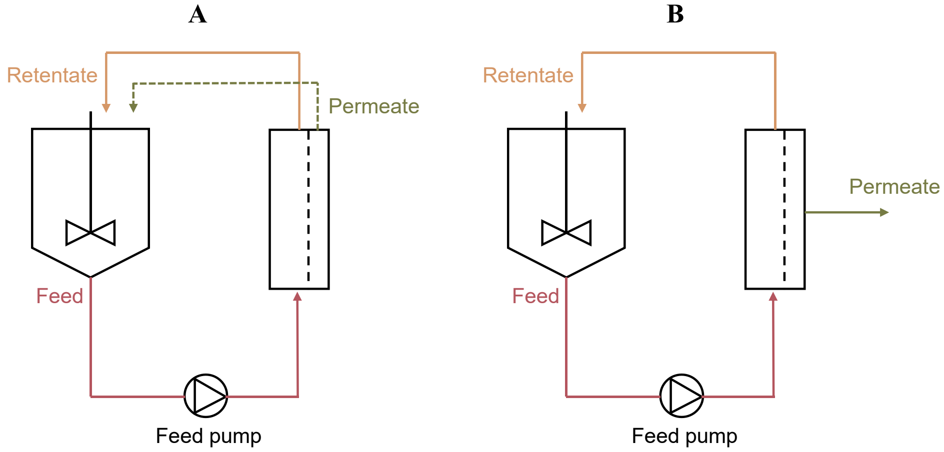

Figure 5: Illustration of a common membrane filtration setup during (A) a parametric study, and (B) a concentration study.

Both parametric and concentration studies were performed in **Papers I** and **II** with NF membranes. Parametric studies were performed to determine the operational parameters that would achieve high lignin retention and high flux. Concentration studies were performed in a constant-pressure mode to determine the extent to which the membranes could concentrate the KBL UF permeate, and how much the flux decreased over time. The filtration experiments performed during the parametric and concentration studies consisted of the following steps: (1) conditioning the membranes, (2) measuring the initial PWF ($PWF_{initial}$), (3) NaOH conditioning (to avoid lignin precipitation on the membrane), (4) filtrating/concentrating the KBL UF permeate, (5) NaOH conditioning, (6) measuring the PWF after filtration of the KBL UF permeate (PWF_{fouled}), (7) cleaning the membranes, and (8) measuring the PWF after cleaning ($PWF_{cleaned}$). The cleaning and PWF measurement steps are detailed in Section 2.2.

During concentration studies, an important parameter is volume reduction, VR, which describes how much permeate volume, V_p, has been withdrawn from the initial feed volume, V_0 (Equation 5). VR is usually expressed as a percentage.

$$VR\ (\%) = \frac{V_p}{V_0} \cdot 100 \qquad (5)$$

Another essential parameter in membrane filtration that was used throughout the research presented in this thesis is retention. In membrane filtration, the goal is generally to concentrate or purify a stream, and so it is important either to have a membrane with high retention, if the desired compound is in the retentate; or that the membrane lets through most of the desired compound while retaining the contaminants, if the desired compound is in the permeate. The true retention, R_{true}, of a compound can be described using Equation 6 [40]:

$$R_{true} = 1 - \frac{C_p}{C_m} \qquad (6)$$

However, it is hard to ascertain the concentration at the membrane surface; therefore, the observed retention, R_{obs}, is used instead [40]. The observed retention is calculated based on the concentration of the solute at the permeate and at the bulk (Equation 7). The observed retention has been expressed in percentage in the results presented in this thesis.

$$R_{obs} = 1 - \frac{C_p}{C_b} \qquad (7)$$

2.2. Fouling and cleaning in membrane processes

Membrane processes are usually designed, run, and improved by trial-and-error studies, in which only the flux and membrane capacity are deciding factors in implementation. Membrane fouling is one of the biggest challenges to industrial implementation of membrane processes [41], but it is uncommon for foulant interactions to be investigated, and for membrane cleaning to be tailored specifically to a specific process [28]. To address these challenges, cleaning and fouling for the NF of KBL UF permeate process were investigated in **Papers III** and **IV**.

The following sections describe membrane fouling and how to monitor and characterise it, and membrane cleaning and how it can be optimised.

2.2.1. Membrane fouling

In the context of membrane filtration, fouling is defined as the "deposition of suspended or dissolved substances – particles, colloids, emulsions, macromolecules and/or salts – on the membrane surface, at the pore openings or within the pores" [32]. Fouling depends on the physical and chemical parameters of the membrane and the feed, such as concentration, temperature, pH, ionic strength, and specific interactions between the compounds in the feed and the membrane surface [42]. Fouling on a membrane is not desirable, as it usually leads to a decline in permeate flux (constant-pressure mode) or an increase in TMP (constant-flux mode), and change in retention over time [29]. It can occur in several forms: adsorption, pore blocking, and cake or gel layer formation (Figure 6) [42].

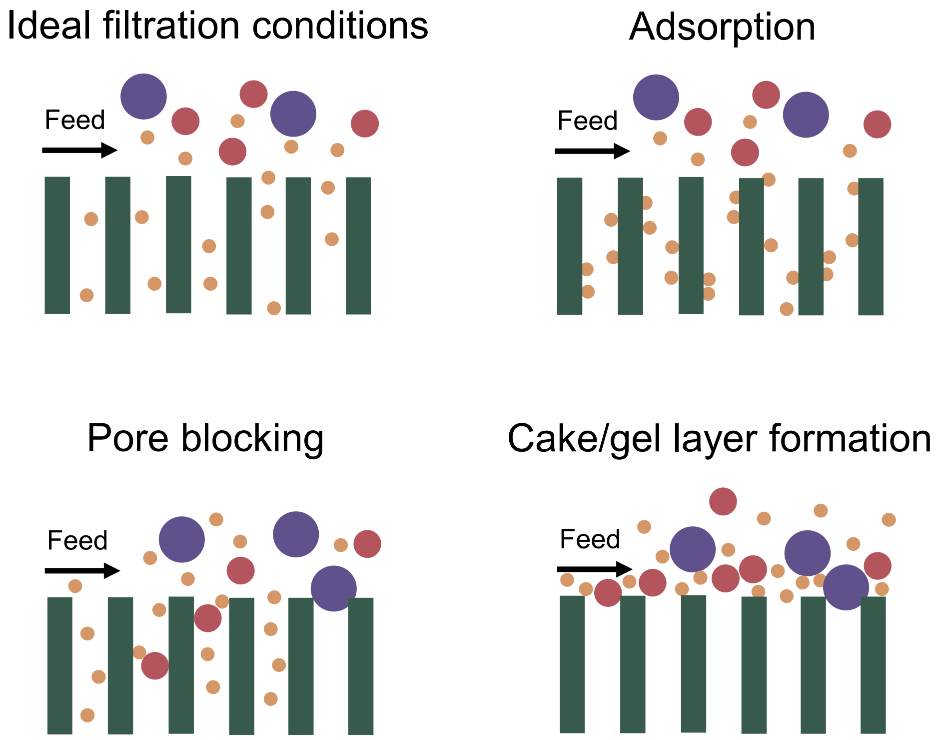

Figure 6: Schematic illustration of ideal filtration conditions and various types of fouling in membrane filtration: adsorption, pore blocking, and cake/gel layer formation.

To model the effect of fouling on the flux, the resistance term in Equation 4 can be expanded to include reversible, R_{rev}, and irreversible, R_{irrev}, fouling, which leads to the resistance-in-series model (Equation 8) [43]. Reversible fouling occurs during the filtration of a solvent, disappears after flushing with water or a water-based solution, and is mainly caused by concentration polarisation. Irreversible fouling occurs due to adsorption and pore blocking, and such fouling can only be removed by cleaning [43].

$$J = \frac{TMP - \Delta\Pi}{\mu \cdot (R_m + R_{rev} + R_{irrev})} \tag{8}$$

Several methods can be used to reduce fouling, including pretreatment of the feed solution, choosing an adequate membrane for the process, optimising the process conditions (such as CFV, TMP, and temperature), and choosing an appropriate module configuration [42]. Although these methods are used to reduce fouling, cleaning is generally needed at some point in the process due to the resulting decrease in flux [42].

Fouling monitoring

Fouling can be monitored using conventional techniques, such as measuring the flux decrease or TMP increase, or *in-situ* monitoring, via optical or acoustic methods [44]. In the research presented in this thesis, various methods were used to study and measure fouling.

The experiments were performed in constant-pressure mode, meaning that it was simple to measure the flux decrease over time using PWF measurements. These were taken every time a filtration experiment was performed, regardless of whether this was part of a parametric or a concentration study, in order to be able to monitor the flux before and after filtration of KBL UF permeate (**Papers I**, **II**, and **III**). For these measurements, the water flux was measured before filtration of the feed ($PWF_{initial}$), after filtration of the feed (PWF_{fouled}), and after rinsing and cleaning the membranes ($PWF_{cleaned}$). These measurements were used to evaluate the quantity of foulants on the membrane after filtration of the feed by calculating the fouling factor (Equation 9):

$$Fouling\ factor\ (\%) = \frac{PWF_{initial} - PWF_{fouled}}{PWF_{initial}} \cdot 100 \qquad (9)$$

PWF measurements can also be used to determine the effectiveness of cleaning in removing the foulants, by calculating the flux recovery (Equation 10).

$$Flux\ recovery\ (\%) = \frac{PWF_{cleaned}}{PWF_{initial}} \cdot 100 \qquad (10)$$

However, PWF measurements do not give any information on the thickness nor the elemental composition of the layer. To get this type of information, *in-situ* monitoring techniques are needed.

One of these techniques is quartz crystal microbalance with dissipation monitoring (QCM-D), which can be used to evaluate the interactions between foulants and surfaces [44,45]. The technique works by placing a piezoelectric quartz crystal on a detector; the sensor oscillates due to electric induction, and the shift in resonance frequency, which is caused by the adsorption and desorption of mass on the sensor surface over time (Figure 7), can be measured. The dissipation is measured when the driving power is interrupted, that is, when there is no electric induction [46]. The frequency and dissipation shifts provide information on mass adsorption and viscoelastic properties [45].

To study fouling processes in membrane filtration using QCM-D, a model membrane surface that represents the real membrane is used. To create a model membrane surface on a quartz sensor, a membrane polymer is spin-coated [47,48] or drop-casted [49] on the surface, or the active layer of a membrane is attached to the sensor [50].

Multiple studies have used QCM-D to investigate membrane fouling. These have focused on protein adsorption in the dairy industry [51,52], biofouling during wastewater treatment [50,53,54], and fouling prevention during water desalination [55], among other subjects. QCM-D can be combined with surface-characterisation techniques, such as atomic force microscopy (AFM), for a fuller understanding of fouling mechanisms [44].

In **Paper IV**, a quartz sensor was coated (using the drop-casting technique) with an NF membrane polymer. The coated quartz sensors were used for QCM-D experiments with the aim of studying the adsorption and desorption behaviour of KBL UF permeate, lignin, and hemicelluloses on the model membrane surface, and better understanding the fouling produced by KBL UF permeate on NF membranes.

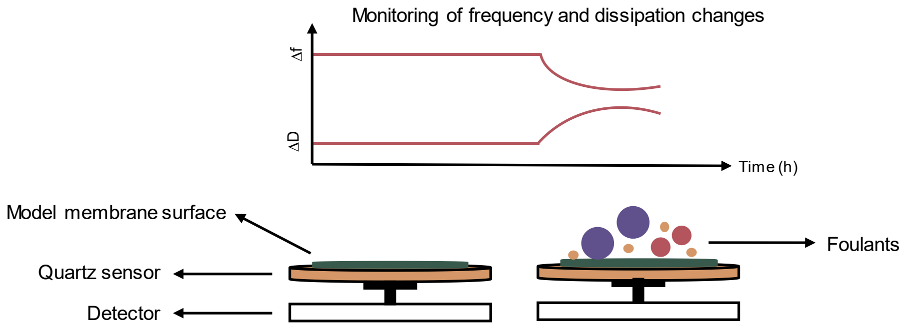

Figure 7: Schematic of QCM-D for *in-situ* monitoring of membrane fouling on a model membrane surface.

Membrane surface analysis and characterisation

Foulants deposited on the membrane surface can be analysed using surface-characterisation techniques such as scanning electron microscopy (SEM), AFM, energy-dispersive X-ray spectroscopy (EDS), and water contact angle (CA). A combination of these techniques is generally used in order to provide a deeper understanding of the membrane surface and fouling.

SEM is largely employed by researchers to characterise the surface properties of a membrane [56]. SEM can provide qualitative information on the shape, size, and arrangement of particles that make up the observed surface, as well as its texture [57]. SEM can be combined with EDS, which provides information on the elemental composition of a sample and map it on its surface [58]. In **Paper III**, SEM-EDS was used to characterise and analyse the chemical composition of the surface of one conditioned, one fouled, and one cleaned membrane.

AFM is commonly used to obtain three-dimensional images of sample surfaces and determine their features at a higher imaging resolution than SEM [59]. It is widely used to characterise membrane surfaces and study membrane fouling, as it can be used to characterise morphology, roughness, and membrane channels [60].

CA measurements can be used to assess the hydrophobicity and fouling tendency of a membrane [61]. A hydrophilic membrane surface is preferred, as this is associated with a low fouling tendency and high water flux [61].

Both CA and AFM were used in **Paper IV** to characterise the model membrane surface that was coated on a quartz sensor.

2.2.2. Membrane cleaning

Cleaning is the process whereby depositions of foreign material on or around the surface of the membrane and in its pores are removed [62]. It is performed at different frequencies depending on the application, generally when the operational flux has decreased to below a threshold value. Cleaning frequency is a critical economic factor, as it has a negative impact on the lifespan of the membrane and requires plant downtime in order to be undertaken [62].

Membrane cleaning can be performed physically or chemically. Physical cleaning involves rinsing the membrane with water at a high or low shear rate, backflushing, and reversing the permeate flux through the pores in order to remove the foulants on the membrane surface [63]. In chemical cleaning, a detergent or cleaning agent is used to remove deposits and restore the initial capacity and separation characteristics of the membrane. The detergent reacts with the fouling layer, breaking down the foulant structures and increasing their solubility [63].

Different types of cleaning agent are used depending on the type of fouling present on the membrane surface [64]. Alkaline cleaning agents are used to remove organic fouling, while acid cleaning agents are used to dissolve precipitations of inorganic salts [65]. Enzymes can be used to break down proteins and remove fat, although they are usually more expensive than conventional chemical cleaning agents [64]. The cleaning agents used should loosen and dissolve the fouling, avoid new fouling, and not attack nor damage the membrane [64]. Other factors to consider when choosing a cleaning agent are how easily it can be rinsed away from the membrane filtration system and its chemical stability, cost, and safety.

Alkaline cleaning agents, namely Ultrasil cleaning agents manufactured by Ecolab AB, were used throughout the research presented in this thesis in order to remove the fouling created by KBL UF permeate. Ultrasil 110 proved successful in removing the organic fouling (**Papers I** and **III**), while Ultrasil 11 combined with Ultrasil 02 recovered the permeate flux well at the pilot plant (**Paper II**).

A cleaning cycle usually consists of the following steps (Figure 8): (1) removing the feed from the membrane filtration equipment, (2) rinsing the system thoroughly with water, (3) cleaning with one or more cleaning agents, (4) removing the cleaning agent from the system with water, and (5) optional disinfection [64].

Figure 8: Schematic showing the steps of a membrane cleaning cycle.

Restoring the initial PWF after cleaning is not always possible, although a low PWF after cleaning may indicate that the cleaning was unsuccessful. The most important factor, however, is that the previous process flux is restored after cleaning [62].

The factors that affect cleaning are usually temperature, time, and the concentration and type of cleaning agent [64]. These factors vary with the type of fouling and membrane material; therefore, choosing adequate cleaning parameters is critical for a successful recovery of the flux.

Optimisation of membrane cleaning

Membrane cleaning is often studied using trial-and-error methods [64]. However, when it comes to optimisation, a systematic approach is needed, and so researchers have turned to Design of Experiments (DoE). This is a statistical methodology that is used for planning, designing, and analysing experiments in a systematic way; process optimisation; and drawing objective conclusions from experiments [66,67]. DoE encompasses several methods or approaches that differ in terms of the number of factors, levels, and responses that are considered. One of these is the response surface methodology (RSM), which is mainly used for modelling and analysing problems when the objective is to optimise the response [66]. Several experimental designs can be used to fit response surfaces, such as central composite designs [68,69]. Central composite designs consider several factors, the values of which vary between low and high. There are three types of central composite design: circumscribed, inscribed, and face-centred.

Central composite designs have previously been used by researchers to optimise membrane cleaning. In some cases, the goal was to predict flux recovery based on the cleaning parameters and cleaning agent used for a specific process and membrane [70,71]. Researchers have also investigated the optimisation of cleaning processes with regard to reducing operating costs and carbon-dioxide emissions [72]. In **Paper III**, a face-centred composite design was used to optimise the cleaning method; three factors – time, temperature and cleaning-agent concentration – each with three levels were studied.

2.3. Lignocellulosic biomass

Lignocellulosic biomass is the most abundant organic component on Earth [73]. The most commonly used lignocellulosic biomass feedstocks in lignocellulosic biorefineries are wood, agricultural crops, and grasses. The lignocellulosic biomass relevant to the research presented in this thesis is wood, which is mainly composed of cellulose, hemicelluloses, and lignin, as well as extractives and ash [74]. Cellulose, hemicelluloses, and lignin are found in the plant cell wall of the wood (Figure 9). In the following sub-sections, each of these components is briefly described.

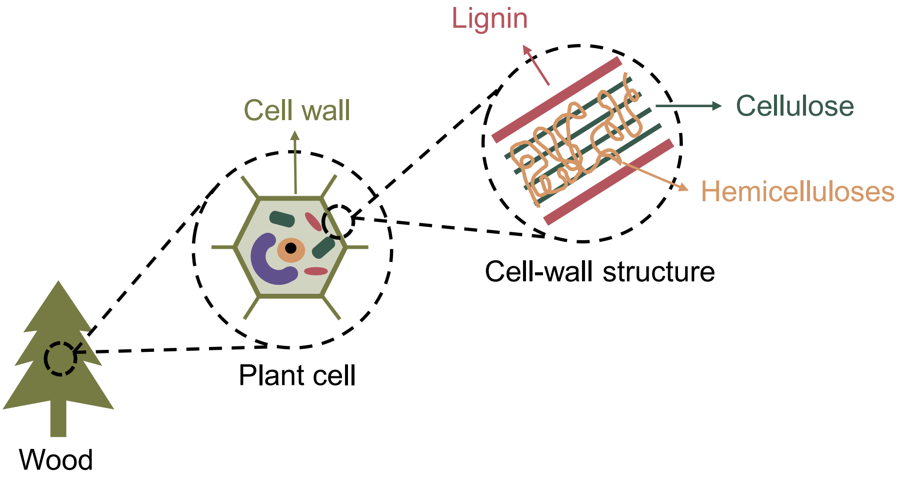

Figure 9: Schematic of the structure of lignocellulosic biomass.

2.3.1. Cellulose

Cellulose is a linear polymer composed of linked glucose units, and contains both crystalline and amorphous parts [75,76]. Cellulose is found on the cell walls of plants, and comprises 40 – 50% of the dry matter in wood [73]. The main goal of pulping is the separation of the cellulose fibres from wood [75]. Because cellulose is stable to chemical attack, both acid and alkaline pulping can be used for that purpose. Cellulose, in the form of chemical pulp, is used to produce paper and paper products; whereas in the form of dissolving pulp is used to produce regenerated cellulose and cellulose derivatives [76].

2.3.2. Hemicelluloses

Hemicelluloses are a group of branched and amorphous polysaccharide polymers, containing pentoses (xylose, arabinose) and hexoses (mannose, glucose, galactose) units [73,74]. Hemicelluloses impart elasticity to wood because they are bonded to other cell-wall components, such as cellulose, cell-wall proteins, lignin, and phenolic compounds [73]. These polymers are not as stable to chemical attack as cellulose, and are partially dissolved in both acid and alkaline pulping conditions [75].

2.3.3. Lignin

Lignin is an aromatic and heterogenous biopolymer, and the second most abundant natural polymer on Earth [77]. Lignin is found in the cell walls and middle lamella of plants, and contributes structurally by gluing cellulose and hemicelluloses together. The lignin content of plants depends on the species, with softwood containing 25 – 35%, and hardwood 15 – 25% [78]. Lignin is formed by three monomers: *p*-coumaryl alcohol (H-unit), coniferyl alcohol (G-unit), and sinapyl alcohol (S-unit) (Figure 10).

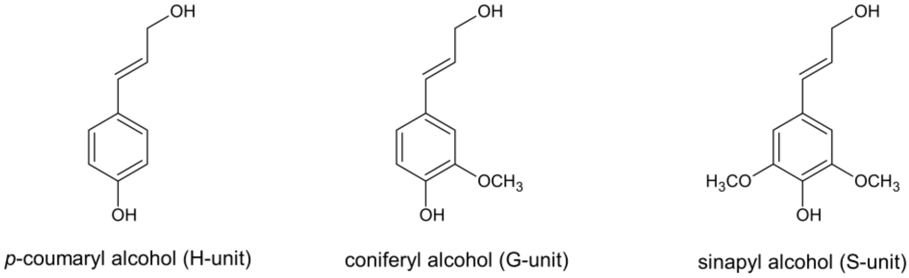

p-coumaryl alcohol (H-unit) coniferyl alcohol (G-unit) sinapyl alcohol (S-unit)

Figure 10: Structure of the three main lignin monomers.

2.4. Kraft pulping process

The most widespread pulping method is the kraft process, which produces roughly 75% of all pulp worldwide. This popularity is due to the high strength and quality of the resulting pulp, high chemical-recovery efficiency of the process, and ability of the method to handle any species of hardwood or softwood [79,80].

The kraft pulping process consists of several steps (Figure 11). When the logs arrive at the mill, they are debarked and chopped into wood chips. The wood chips are then loaded into the digester (pulping step), where they are submerged in warm white liquor that is composed of sodium hydroxide (NaOH) and sodium sulphide. The digester contents are heated to 160 – 170ºC, and this cooking temperature is maintained until the desired degree of delignification is achieved [75]. The goal of pulping is to liberate the cellulose fibres by removing lignin from the cell wall and middle lamella of the wood [75]. Hemicelluloses are also dissolved and degraded into acid groups during the pulping process. The cellulose fibres are separated from the liquor in the washing step, and the pulp is then either sent to the bleaching step or proceeds directly to paper production.

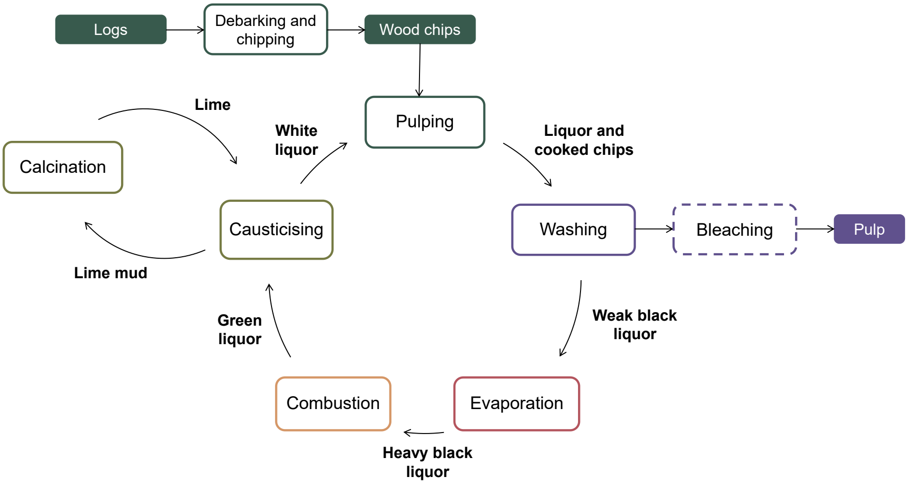

Figure 11: Kraft pulping process and chemical-recovery cycle.

The weak black liquor that exits the washing step then enters the kraft chemical-recovery cycle; here, it is concentrated in multi-effect evaporators (evaporation step) to produce heavy black liquor, which has a concentration of solids of 65% or higher, allowing it to be burned in the recovery boiler (combustion step) [80]. Incinerating the heavy black liquor produces an inorganic smelt of sodium carbonate and sodium sulphide, which flows out of the furnace and enters the smelt dissolving tank, where it is dissolved in water to form green liquor [75]. The green liquor is converted into white liquor by a causticising plant, where it reacts with lime to convert the sodium carbonate into NaOH and calcium carbonate (causticising step) [81]. The calcium carbonate is removed as lime mud and regenerated by burning in a lime kiln (calcination step) [81], while the sodium sulphide passes through this process unchanged. The white liquor is returned to the digester to be reused in the pulping step.

The heat that results from black liquor combustion is recovered as high-pressure superheated steam [80], which is passed through a steam turbine to generate process steam. This can in turn be used in various processes in the mill [81].

2.4.1. Separation of lignin from kraft black liquor

The kraft pulping process was invented in 1879, and has been constantly improved since [81]. In recent decades the focus has been on improving the economic and environmental performance of pulp mills, which are limited by the chemical-recovery step of the process due to the recovery boiler being the bottleneck of mills [82]. This is due to the constant increase in the production of pulp and, consequently, of black liquor, which slows down the combustion of heavy black liquor, preventing mills increasing production.

One of the proposed solutions to this problem is removing or separating lignin from the black liquor [83] to decrease its organic content, reducing the load on the recovery boiler [84]. This would allow pulping production to be increased without the need to invest in a larger recovery boiler. In addition to improving the efficiency of pulping, kraft lignin can be used to produce biofuel and value-added products [85]. Applications for kraft lignin include additives for concrete mixtures, dust control, feed and food additives, dispersants, resin and binder compositions, emulsifiers, and rubber additives [86].

One way to remove or separate lignin from black liquor is precipitation, with precipitation by acidification being the most common method of extracting lignin from KBL. Here it is usual for carbon dioxide, sulphuric acid, or waste acid from the bleaching step in the mill to be used to decrease the pH of the black liquor, causing the lignin to precipitate [87]. Kraft lignin obtained from precipitation was first commercialised by Ingevity (formerly MeadWestvaco) in 1942 [88]. Other precipitation methods have been developed since, such as the LignoBoost process, invented by Chalmers University of Technology and Innventia (currently part of Research Institutes of Sweden; RISE) and now owned by Valmet. The LignoBoost process produces a solid lignin with 1% ash and 65 – 70% dryness, thanks to a two-stage process [83,89,90].

Another solution that has gained interest in recent years is lignin fractionation by membrane filtration. Membrane technology is economically and environmentally beneficial for the recovery of lignin, as membranes facilitate lignin separation without the need for pH or temperature adjustment [91], and it is possible to control the molecular weight of the lignin fraction by using membranes with different MWCOs [13]. Nevertheless, membrane processes have not yet been commercialised in relation to the recovery of lignin, and further research is needed to scale up the process.

3. Current work – Nanofiltration of kraft black liquor ultrafiltration permeate

As is discussed in Sections 1.1 and 2.4, membrane processes can be used to separate lignin from KBL. The research presented in this chapter examined the possibility of implementing an NF step after a UF step during the filtration of KBL, in order to extract lignin and produce a permeate with a low quantity of organics that could be reused in pulp and paper mills.

This chapter discusses different aspects that need to be considered when such a process is developed and optimised. These aspects are: choosing a membrane and operating conditions, establishing a cleaning procedure that successfully recovers the flux, studying the foulants in the feed, and understanding the costs of the process.

3.1. Kraft black liquor ultrafiltration permeate

The feed solution used in the four studies that are part of this thesis (**Papers I – IV**) was KBL UF permeate (Table 2). The composition of the KBL UF permeate used in the pilot studies (**Paper II)** was slightly different from the one presented here, as it was produced at a different time, with the main differences being a lower total hemicelluloses concentration and a higher ash content.

To obtain the UF permeate, KBL was filtered using a 1 kDa UF ceramic membrane, manufactured by Alsys Kleansep (Salindres, France). The KBL was a mixture of 70% softwood and 30% hardwood. The UF step was performed by SunCarbon AB (Piteå, Sweden) using a membrane pilot plant located at a pulp and paper mill in Sweden, which was set up to extract lignin.

Table 2: KBL UF permeate composition and properties.

pH	13.13 ± 0.08
Viscosity at 50°C (mPa·S)	1.00 ± 0.06
Viscosity at 70°C (mPa·S)	0.82 ± 0.07
Density (g/L)	1.07 ± 0.01
Molecular weight (Da)	1564.2 ± 47.2
Total solids (g/L)	199.1 ± 2.4
Ash (g/L)	73.6 ± 1.4
Total hemicelluloses (g/L)	2.01
Arabinose (g/L)	0.44 ± 0.05
Galactose (g/L)	1.19 ± 0.05
Glucose (g/L)	0.11 ± 0.03
Xylose (g/L)	0.27 ± 0.05
Total lignin (g/L)	29.7 ± 0.8
Klason lignin (g/L)	22.8 ± 0.3

3.2. Laboratory-scale experiments

The first stage in the development of the NF step was selecting an adequate commercial membrane at laboratory scale. Two essential steps were performed: (1) testing several pre-selected commercial membranes in parametric studies, and (2) testing the best performing membranes from the parametric studies in concentration studies to further assess their potential. The results presented in this section come from the work performed in **Paper I**.

3.2.1. Membrane screening

The first step was to select and test several commercial NF membranes that are able to withstand the high pH of the KBL UF permeate and operate in the temperature range of 50 – 70°C. Thus, ten commercially available NF membranes were selected to test them in parametric studies (Table 3).

Table 3: NF membranes and their characteristics. MWCO values are as specified by the manufacturer in the data sheet for each membrane.

Membrane name	Manufacturer	Type	MWCO (Da)
MexFil MP025 dNF40	NXFiltration	Hollow fibre	400
UF-pHt GR95PP	Alfa Laval	Flat sheet	2000
NADIR NP030 P	MANN+HUMMEL Water & Fluid Solutions	Flat sheet	500-600
NADIR NP010 P	MANN+HUMMEL Water & Fluid Solutions	Flat sheet	1000 – 2000
SelRO MPF-36	Koch Separation Solutions	Flat sheet	1000
SelRO MPF-34	Koch Separation Solutions	Flat sheet	200
NF090801	SolSep BV	Flat sheet	350
NanoPro B-4021	AMS Technologies	Flat sheet	100
NanoPro B-4022	AMS Technologies	Flat sheet	150
LC1	Inopor	Tubular ceramic	200

The flux at each TMP point was plotted for the ten membranes tested (Figure 12). The membranes with the highest fluxes were the NADIR NP010 P and the ceramic LC1. The membranes with the lowest flux were the NanoPro B-4021, NanoPro B-4022, and SelRO MPF 34, which did not start producing permeate until a TMP of 20 – 25 bar was reached. These membranes were among those with the smallest pore size, which could explain their low permeate flux.

For all of the membranes, increasing the TMP increased the flux, with some of the membranes approaching their limiting flux at higher TMPs. The GR95PP exhibited such a behaviour after 20 – 25 bar, and the SelRO MPF-36 and NADIR NP010 P after 30 – 35 bar, at which point the flux curves seemed to start to flatten.

Lignin retention was plotted against the tested TMPs for the ten membranes (Figure 13). For most of the membranes, lignin retention increased with increasing TMP, which can be explained by the increasing TMP causing the flux to increase, and increasing flux causing the concentration polarisation to increase. This in turn caused an increase in the transport of solvent through the membrane, which in this case was mainly water. Thus, the amount of solvent in the permeate was higher compared to the amount of solute, while the concentration at the membrane increased due to convective transport. Therefore, the retention of solutes, in this case lignin, increased. Compaction of the membrane may also have played a role in the increased retention at higher TMPs.

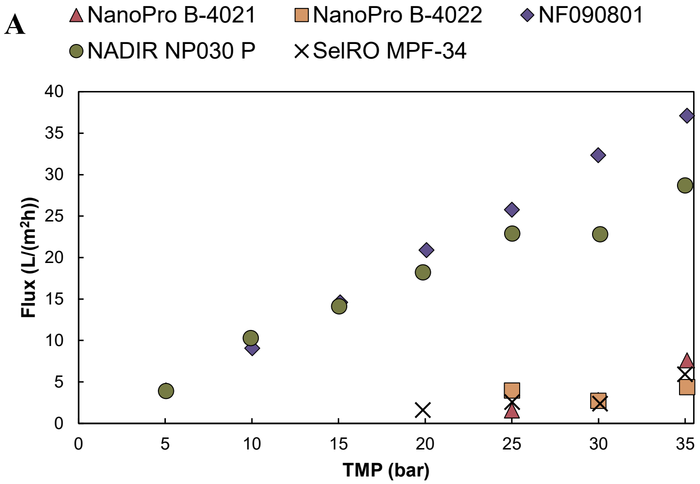

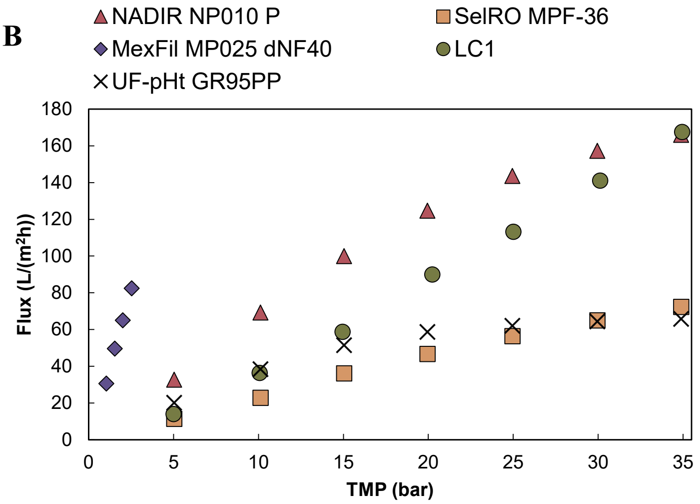

Figure 12: Flux vs. TMP during the parametric studies for (A) NF090801, NanoPro B-4021, NanoPro B-4022, NADIR NP030 P, and SelRO MPF-34; and (B) MexFil MP025 dNF40, NADIR NP010 P, SelRO MPF-36, LC1, and UF-pHt GR95PP.

The highest lignin retentions were achieved at a TMP of 35 bar. At this TMP, both the NanoPro B-4022 and SelRO MPF-34 had lignin retention greater than 95% (Figure 13A). The lowest lignin retention was achieved by the hollow-fibre MexFil MP025 dNF40, which could not be tested at the same TMPs as the flat-sheet and tubular ceramic membranes due to the pressure limitations of the housing (Figure 13B).

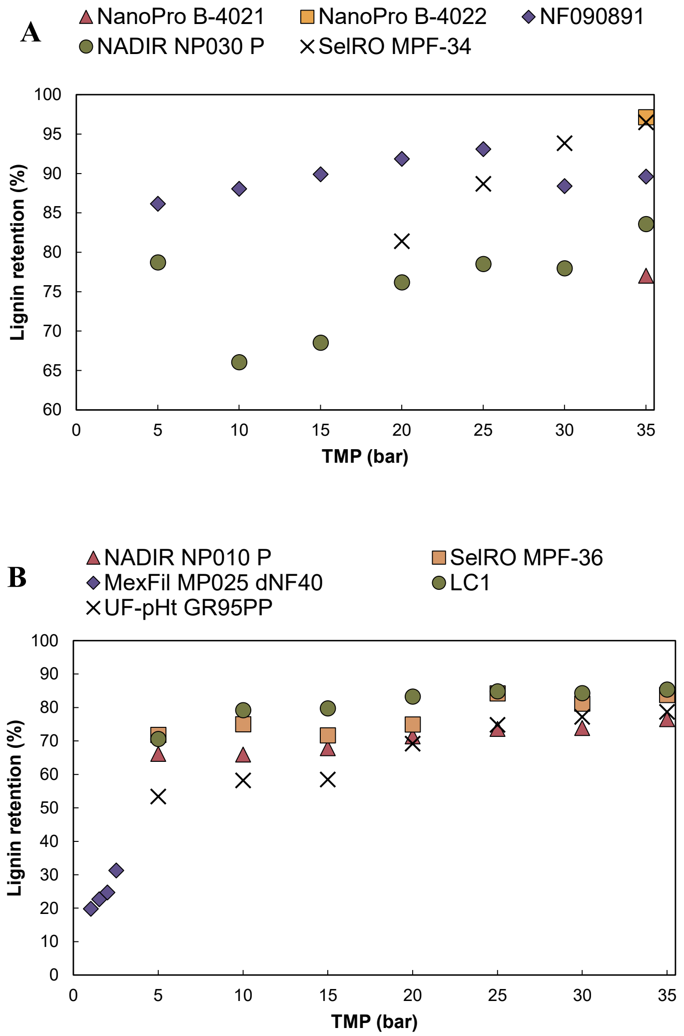

Figure 13: Lignin retention vs. TMP during the parametric studies for (A) NF090801, NanoPro B-4021, NanoPro B-4022, NADIR NP030 P, and SelRO MPF-34, and (B) MexFil MP025 dNF40, NADIR NP010 P, SelRO MPF-36, LC1, and UF-pHt GR95PP.

The membranes with the combinations of flux and lignin retention that were judged to be the best were the LC1, SelRO MPF-36, and NF090801. These three membranes had lignin retention of over 80%, in combination with medium to high flux (Table 4).

Table 4: Average lignin retention and flux for the LC1, SelRO MPF-36, and NF090801 membranes.

Membrane	Average lignin retention (%)	Average flux (L/(m^{2}h))
LC1	81	89
SelRO MPF-36	78	44
NF090801	90	21

The LC1 membrane seemed to be the obvious candidate for pilot scale, but is a semi-commercial membrane that at that time was still under development. Therefore, the MWCO of the membrane was tested by filtering a polyethylene glycol (PEG) solution before and after the KBL UF permeate. The PEG was not retained to the same degree at the beginning and end of the filtration, as can be seen by the peak at 1000 Da (Figure 14). This means that the MWCO of the membrane was not stable during the filtration process.

Based on these results, the LC1 membrane was not considered for further evaluation, even though ceramic membranes are better at withstanding higher temperatures and pH than polymeric membranes, and can operate at higher TMPs. Therefore, the two polymeric membranes SelRO MPF-36 and NF090801 were chosen for further study of their concentration performance with KBL UF permeate.

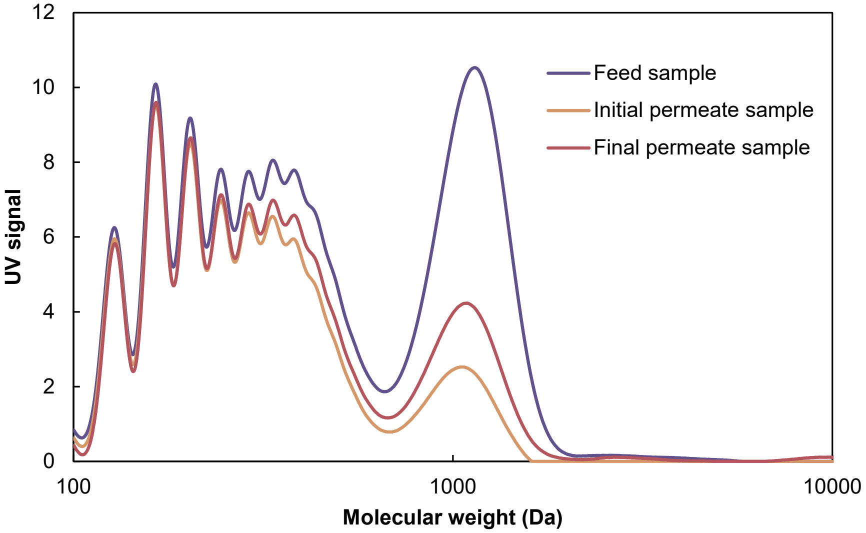

Figure 14: Molecular weight distribution of a PEG solution that was filtrated through the LC1 membrane. Data is shown for the feed sample, and for the permeate samples obtained before (initial permeate sample) and after (final permeate sample) NF of KBL UF permeate.

3.2.2. Concentration study

The selected membranes SelRO MPF-36 and NF090801 were used in a concentration study to evaluate their performance under the following two conditions: (A) 50°C and 35 bar, and (B) 70°C and 15 bar, both at a CFV of 0.5 m/s. Condition A was chosen because these conditions resulted in the best combination of flux and lignin retention for the selected membranes during the parametric study. Condition B was selected because, at pilot scale, the KBL UF permeate exits the UF step at 97ºC. Hence, for the NF step to be performed afterwards, the permeate will have to be cool down to either 50ºC or 70ºC. If the membranes can operate at 70ºC, energy for cooling can be saved. Moreover, the feed has a lower viscosity at higher temperatures, decreasing the resistance of transport.

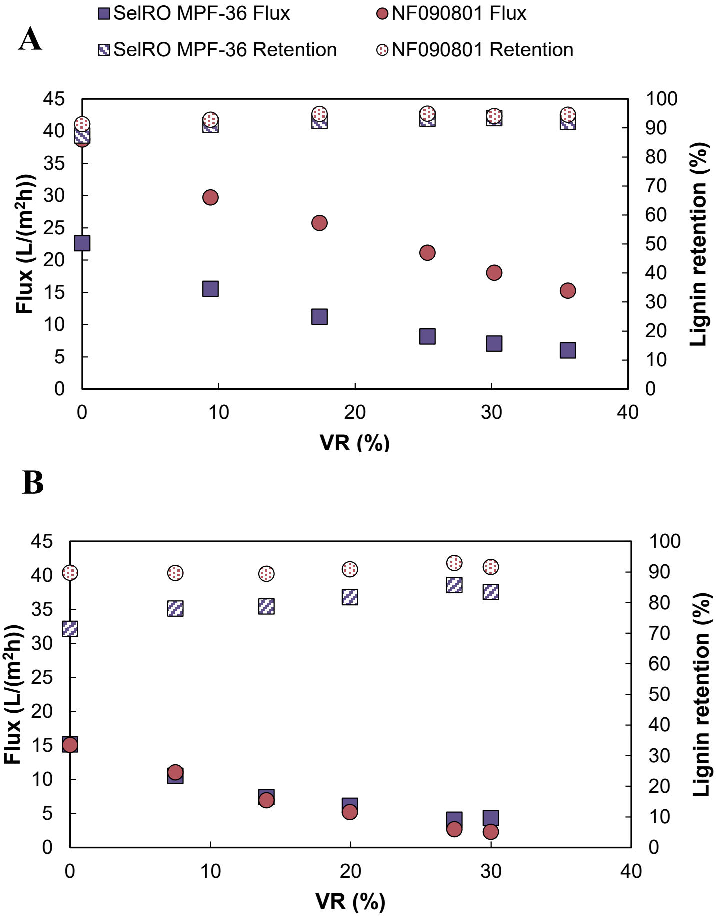

Figure 15: Flux and lignin retention vs. VR during the concentration study performed to investigate (A) Condition A, 50°C and 35 bar, and (B) Condition B, 70°C and 15 bar.

The flux and lignin retention were measured at regular intervals as the VR increased (Figure 15). The concentration test that investigated Condition A reached a VR of 35% (Figure 15A), whereas the concentration test that investigated Condition B ended at a VR of 30% (Figure 15B).

NF090801 and SelRO MPF-36 both had high lignin retention under Condition A (Figure 15A). However, NF090801 had a much higher flux throughout the test. For Condition B, both membranes had similar fluxes for the duration of the test (Figure 15B), but NF090801 had a higher lignin retention (90 – 92%) than SelRO MPF-36 (71 – 89%).

The molecular weight distributions of one feed sample and two permeate samples (one produced by each membrane) at a VR of 35% were analysed (Figure 16). This was undertaken in order to evaluate the lignin-fractionation capacity of the membranes. Both membranes were successful in separating the lignin into different molecular weight fractions. The feed sample had a molecular weight of 1419 Da, the permeate sample obtained with the NF090801 membrane had a molecular weight of 666 Da, and that obtained with the SelRO MPF-36 membrane had a molecular weight of 757 Da. This indicates that the permeate produced by the NF090801 membrane had an overall lower molecular weight than that produced by the SelRO MPF-36 membrane.

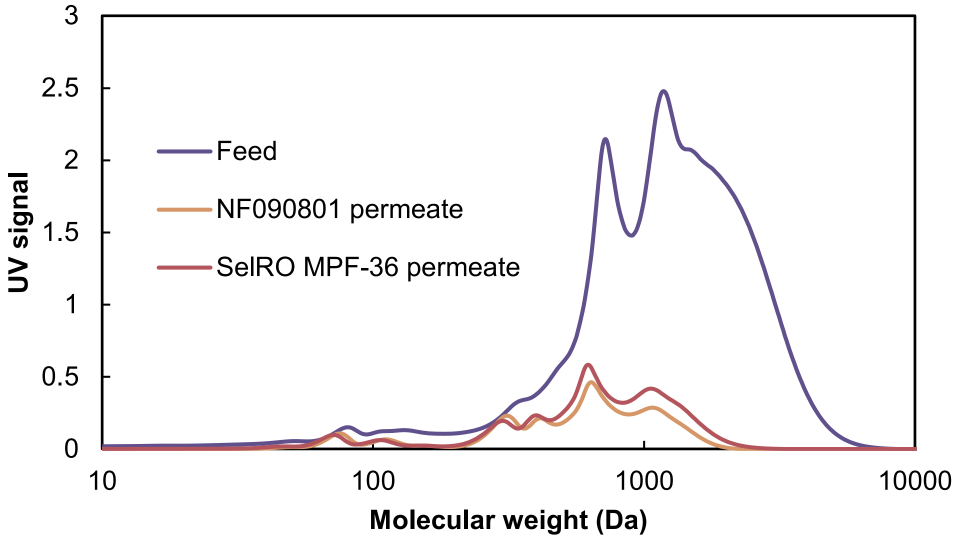

Figure 16: Molecular weight distribution of the feed, the NF090801 permeate, and the SelRO MPF-36 permeate at a VR of 35% during the concentration test under Condition A.

3.3. Pilot-scale concentration study

The next stage of the development of the NF step was testing whether the chosen membrane (NF090801) had the same performance at both laboratory and pilot scale. Therefore, pilot-scale experiments were performed using a membrane filtration plant located at an integrated pulp and paper mill in the north of Sweden. The NF090801 membrane in a spiral-wound configuration was used to perform these experiments. The results presented here are from **Paper II**.

For the pilot-scale study, the two investigated conditions were adapted to the limitations of the membrane pilot plant, and were: (A) 50ºC and 25 bar, and (B) 70ºC and 15 bar. The conditions were run twice each, in the order A1 → B1 → A2 → B2, and the flow was set to 1 m^3/h. The membrane had a filtration area of 1.8 m^2.

3.3.1. Flux results

The fluxes were plotted against VR for the four tests performed (Figure 17). A VR of 80% was achieved for each of the tests performed; however, concentration was achieved more quickly under Condition B compared to Condition A (Table 5). Test A1 took 4.5 hours to reach a VR of 80%, while test B2 took 3 hours to reach the same VR.

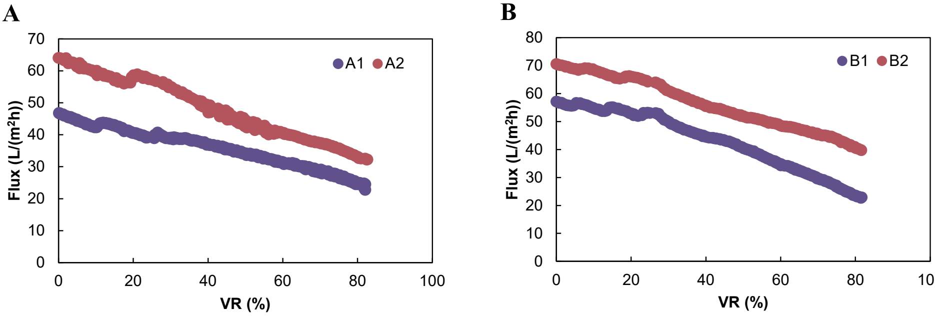

Figure 17: Flux vs. VR for the concentration tests performed at (A) 50ºC and 25 bar, and (B) 70ºC and 15 bar.

The shorter time to achieve concentration for Condition B compared to Condition A is directly linked to the average flux; a higher flux was observed under Condition B than Condition A. This was because the viscosity of the KBL UF permeate at 70ºC was lower than at 50ºC (Table 1), resulting in a higher flux during filtration at 70ºC.

Table 5: Average flux and time to reach a VR of 80% for the four concentration tests performed at pilot scale.

Test	Average flux (L/(m^{2}h))	Time to reach VR of 80% (h)
A1	35	4.5
A2	46	3.5
B1	40	4.0
B2	55	3.0

It was expected that tests performed under the same conditions would have similar fluxes, and that tests A1 and A2 would have lower fluxes than B1 and B2. However, the average flux increased in the order that the tests were performed, i.e. A1 → B1 → A2 → B2. A possible reason for the constant increase in flux is that the operating temperature at which the tests were performed (70ºC) was too high for the membrane. If this hypothesis is correct, the membrane was damaged after concentration at 70ºC during Test B1, increasing the flux for Test A2.

The operating TMP was set higher for Condition A compared to Condition B; however, temperature seemed to be the operating condition that affected the flux the most. Usually, an increase in TMP means an increase in flux, but in this case the membrane had a lower flux at 25 bar (Condition A) compared to 15 bar (Condition B).

3.3.2. Lignin, total solids, and ash retention

Samples taken at VRs between 0% and 80%, increasing in increments of 10%, were analysed for lignin, total solids (TS), and ash. Overall, the average values for lignin retention were 70 – 80%, for TS retention 15 – 25%, and for ash retention 10 – 20% (Figure 18).

Under Condition A, lignin retention was slightly higher, with averages of 82% for A1 and 77% for A2; under Condition B, these were 75% for B1 and 70% for B2. Hence, lignin retention decreased with increasing operating temperature. Mänttäri et al. also observed a decrease in retention when testing NF membranes for glucose retention at increasing temperatures [92]. Their explanation for this was that the diffusion of inorganic and organic substances increased with higher temperature, which is also a possible explanation in this case.

The TS retention followed the same trend as the lignin retention, based on the average values (Figure 18). Test A1 had the highest average TS retention (25%), followed by Tests B1 and B2 (22% and 19%, respectively). Test A2 was expected to have a similar TS retention to Test A1, but had the lowest value (14%).

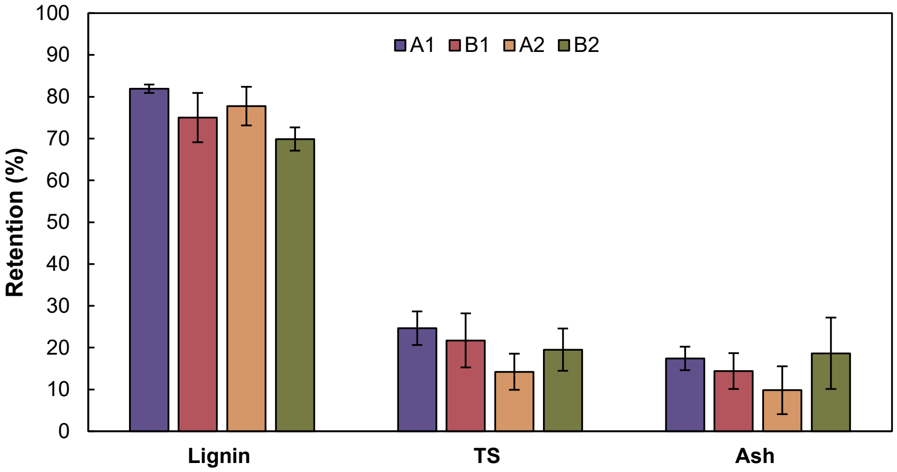

Figure 18: Average retention of lignin, TS, and ash, with the corresponding standard deviation for NF of KBL UF permeate for the four concentration tests performed.

Ash retention fluctuated between 0 and 20% at 50ºC, and between 0 and 30% at 70ºC (Figure 19). Tests A2 and B2 had large standard deviations, showing that ash retention was not stable over time.

The differences in TS and ash retention for tests performed under the same operating conditions, and the increase in the standard deviation of Tests A2 and B2, may have been caused by temperature cycling (50ºC → 70ºC → 50ºC → 70ºC). According to Yao et al., increasing the temperature from 25 to 50ºC increases the permeate flux and reduces the separation performance of polymeric membranes with MWCOs of smaller than 2000 Da [93]. They concluded that when the operating temperature returned to 25ºC, the separation performance returned to the original value as the reduction was not permanent, and that no permanent changes in membrane morphology occurred. In the tests presented in this section, the higher operating temperature may have damaged the membrane, causing a permanent change in its morphology, as can be seen from the reduction in retention after operation at 70ºC. This caused a non-uniform retention over the whole membrane surface, which changed over time during filtration, giving a large standard deviation. Returning to the lower operating temperature did not return the retention and flux to the initial values.

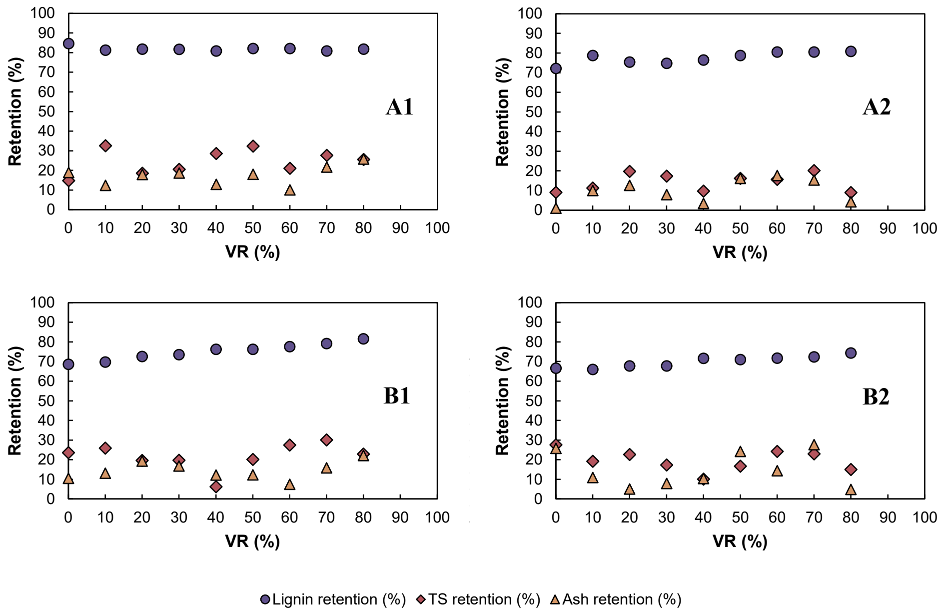

Figure 19: Lignin, TS, and ash retention vs. VR for the four concentration tests performed at pilot scale.

3.3.3. Pure water flux measurements and membrane cleaning

During the pilot studies, $PWF_{initial}$, PWF_{fouled}, and $PWF_{cleaned}$ were measured (see Section 2.2.1. for more information). Thereafter, the permeability (L/(m^2·h·bar)) was calculated by dividing the flux by the TMP at which it had been measured. Then, the normalised permeability was calculated by dividing each permeability by the initial permeability (Figure 20).

The initial normalised permeability for every test was 1, which facilitated evaluation of the decrease (or increase) in permeability following KBL UF permeate filtration and cleaning. For Tests A1, A2, and B2, the permeabilities were reduced by 30 – 40%, whereas for Test B2 the permeability was only reduced by 13%. For Tests A1 and B1, the alkaline cleaning successfully recovered the flux, as the permeability after cleaning was higher than 0.8. However, for Tests A2 and B2, the permeabilities after cleaning were higher than 1. This indicates that either the filtration or cleaning damaged the membrane, as the flux after cleaning was higher than the initial flux. This is in line with the flux and retention results presented above, where flux increased and retention decreased from the first to the last test.

Other studies have observed an increase in permeability after cleaning. One concluded that the feed had modified the membrane during filtration, and that this was the cause of an observed increase in permeability after cleaning [94]. The results presented in this thesis seem to be similar, although those authors did not identify any membrane damage. Another study found that the flux increased after cleaning with an alkaline cleaning agent [92]. In the research presented in this thesis, cleaning was also performed with an alkaline cleaning agent, which could have contributed to the increase in flux after cleaning. Most likely, a combination of high-temperature operation with a high pH solution and the use of an alkaline cleaning agent changed the morphology of the membrane and damaged the membrane surface. This led to a decrease in retention and an increase in flux and water permeability in the last tests performed.

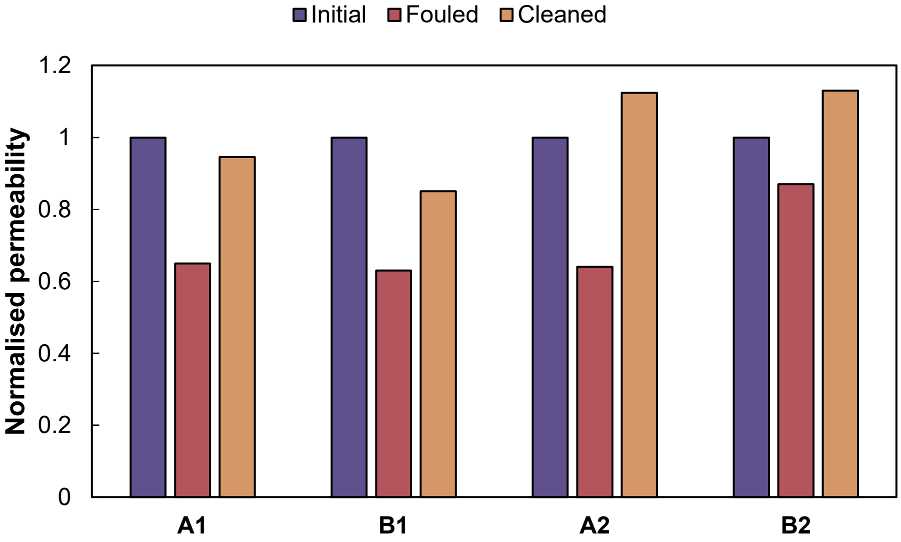

Figure 20: Normalised permeability for the three PWF measurements performed for each concentration test.

In conclusion, operation at 70ºC at pilot scale was not satisfactory, and all analysis and data point to a change in membrane morphology and damage to the membrane surface. In contrast, concentration of KBL UF permeate at 50ºC and 25 bar had a high lignin retention and reasonable average flux. Moreover, cleaning with an alkaline cleaning agent was able to successfully recover the flux to 80% of its original value. Therefore, the results from Test A1 were used in the techno-economic analysis presented in Section 3.6, where the technical potential and economic feasibility of this process are discussed.

3.3.4. Comparison between laboratory and pilot-scale results

The results of the laboratory and pilot-scale experiments were expected to be different as regards both flux and lignin retention, due to differences in operating conditions, the type of membrane used (flat sheet vs. spiral-wound module), and membrane equipment. Additionally, the feed for the pilot study was produced immediately before the concentration studies, while the feed used in the laboratory study was produced several months before the experiments took place. This difference in when the feeds were produced resulted in changes in composition, as the composition of wood changes over time in pulp mills, hence changing the composition of the KBL used in the UF step.

The average lignin retention was higher during the laboratory-scale experiments, whereas the average flux was higher during the pilot-scale experiments (Table 6). Temperature had a larger impact at the pilot scale than the laboratory scale, possibly due to heating and insulation of the membrane equipment. At laboratory scale, only the tank was heated, whereas at pilot scale there were heat exchangers that ensured that the KBL UF permeate stayed at the desired temperature throughout filtration.

Table 6: Average lignin retention and average flux for the concentration tests at laboratory and pilot scale.

Experiment scale	Operating conditions	Average lignin retention (%)	Average flux (L/(m^{2}h))
Laboratory	50°C, 35 bar	93.8 ± 1.3	24.8
	70°C, 15 bar	90.8 ± 1.2	7.2
Pilot	50°C, 25 bar	79.7 ± 3.0	40.7
	70°C, 15 bar	72.4 ± 4.3	47.6

However, at laboratory scale the pressure may have had a greater impact on the flux, as higher TMP results in higher flux. In contrast, at pilot scale the pressure seemed to have little impact compared to temperature, as the flux was higher at a TMP of 15 bar than at a TMP of 25 bar.

Overall, the results produced at pilot scale demonstrated that it is possible to scale up the NF step. Although the lignin retention was not as high as at laboratory scale, an average lignin retention of 80% can be achieved. In addition, it was shown that a higher flux can be achieved at pilot scale than at laboratory scale.

3.4. Membrane-cleaning optimisation

For the successful application of an NF step in the treatment of KBL UF permeate, a membrane-cleaning method that recovers the flux after the membrane has been fouled must be designed and implemented. Ideally, the cleaning method would use low quantities of water and cleaning agent, and be performed in a short time. To this end, the membrane-cleaning method for the NF step of treating KBL UF permeate was optimised using an RSM approach. The results presented here are from **Paper III**.

3.4.1. Experimental design

An RSM with a face-centred composite design was chosen for optimising membrane cleaning and investigating the interactions between the factors. The three factors studied were temperature (T), time (t), and cleaning-agent concentration (C). Each factor had three levels: low (-1), centre (0), and high (+1) (Table 7). The response factor was the flux recovery, which was used to evaluate the efficiency of the cleaning. The cleaning agent chosen was Ultrasil 110, which is an alkaline cleaning agent.

Table 7: Factors studied, symbols, and level details for each factor.

Factor	**Symbol**	**Level details**		
		Low (-1)	**Centre (0)**	**High (+1)**
Temperature (ºC)	T	30	40	50
Time (min)	t	30	45	60
Cleaning agent concentration (wt%)	C	0.05	0.5	1.0

Using the levels of the three factors and determined response factor, a set of cleaning methods was created using the MODDE 13 Pro DoE software (Sartorius, Göttingen, Germany).

In total, 17 experiments were performed; membranes that had been fouled using KBL UF permeate were cleaned using varying permutations of the three factors (Table 8). The detailed steps for each experiment are presented in Section 2.1.3.

Table 8: Face-centred composite design matrix for the cleaning methods, detailing the conditions under which each was to be performed.

Cleaning method	Temperature (°C)	Time (min)	Cleaning-agent concentration (wt%)
1	50	60	1.00
2	50	30	1.00
3	30	30	1.00
4	50	45	1.00
5	50	60	0.50
6	50	45	0.50
7	30	60	0.05
8	50	30	0.50
9	50	45	0.05
10	30	60	1.00
11	30	45	0.50
12	40	30	0.50
13	30	30	0.05
14	40	45	0.05
15	40	45	1.00
16	40	45	0.50
17	40	45	0.50

3.4.2. Model development and validation

Flux recovery was calculated using the data from the PWF measurements for each of the cleaning methods (see Section 2.2.1.). Using the calculated flux recoveries and cleaning-method permutations, a quadratic response surface model (Equation 11) was obtained by statistical analysis (for more details, see **Paper III**):

$$Y_{flux\ recovery\ (\%)} = -99.5845 + 10.7583 \cdot T - 0.949898 \cdot t - 64.0058 \cdot C - 0.152328 \cdot T^2 - 92.277 \cdot C^2 + 2.34029 \cdot T \cdot C + 1.94399 \cdot t \cdot C \quad (11)$$

Using this model, the flux recovery was predicted for each cleaning method. To assess whether the model was able to successfully predict flux recovery based on the cleaning factors, the differences between the observed and predicted data were used. The coefficient of determination, R^2, indicates how well a model fits experimental values; the closer the value is to 1, the better the fit. For the model developed, R^2 was 0.75, indicating that the model fits the experimental data well (Figure 21).

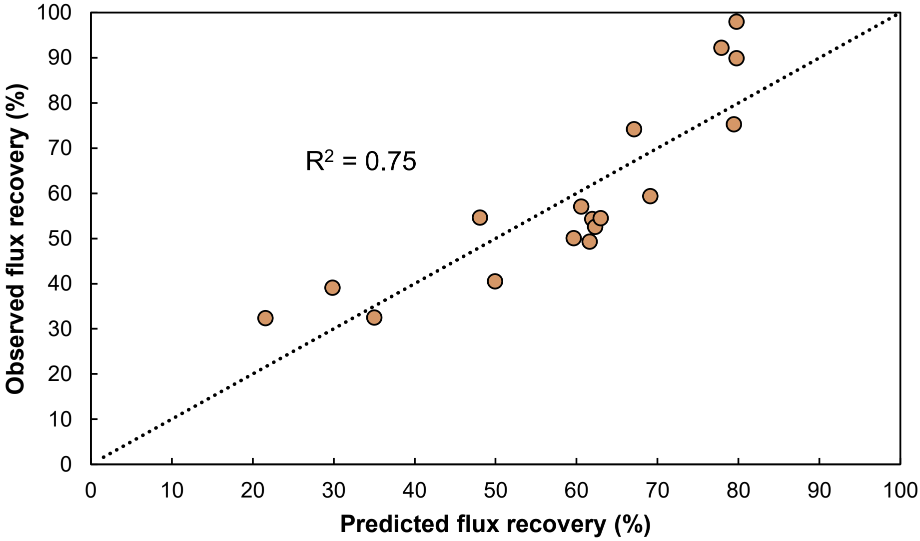

Figure 21: Observed vs. predicted flux-recovery values.

The developed model was used to investigate the interactions between the cleaning factors. To this end, the model was plotted in 4D contour plots that show how each factor influenced the response, i.e. flux recovery (Figures 22 and 23).

Cleaning for 30 minutes yielded a maximum flux recovery of between 70 and 80%. When the time was increased from 45 to 60 minutes, the area of the countour plot where a flux recovery of greater than 80% was obtained increased (Figure 22). Increasing cleaning time has been shown to be effective in increasing cleaning efficiency [95], since the cleaning solution has more time to interact with the foulants.

Increasing the cleaning temperature usually leads to an increase in flux recovery [95], but this was not the case in this study; here, at temperatures of up to 49ºC, flux recovery higher than 80% was obtained (Figure 22C). However, at 50ºC, the highest range that could be obtained for the flux recovery was 70 – 80% (Figure 23C). Thus, it was concluded that a temperature of 34 – 49ºC is adequate for performing the cleaning.

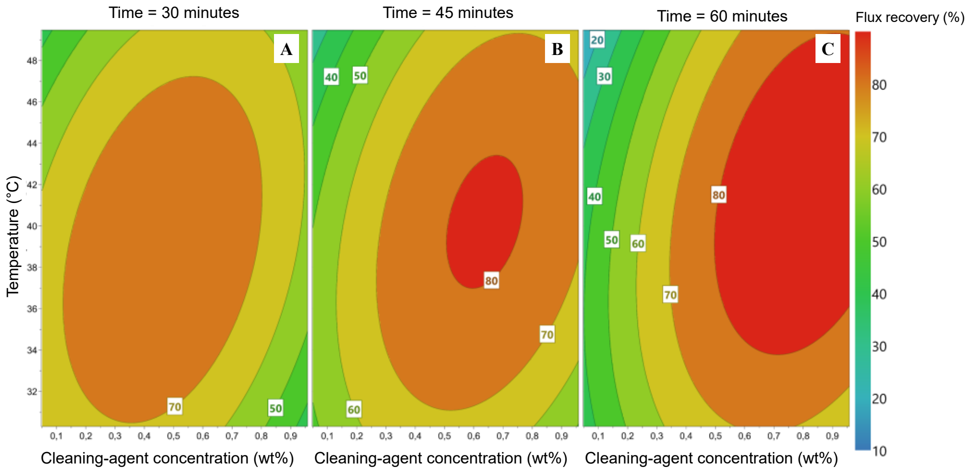

Figure 22: 4D contour plots showing temperature vs. cleaning-agent concentration at (A) 30 minutes, (B) 45 minutes, and (C) 60 minutes of cleaning.

When the cleaning time was more than 45 minutes, cleaning-agent concentrations greater than 0.5 wt% did not impact flux recovery. For 60 minutes of cleaning, for example, the range of cleaning-agent concentration that was able to achieve a flux recovery of greater than 80% was 0.5 – 1 wt%; for 45 minutes of cleaning, the range was smaller, at 0.5 – 0.8 wt%. A similar effect was reported by Mohammadi et al., who found that increasing the concentration of NaOH (used as cleaning agent) up to 0.8 wt% increased the flux recovery considerably, but the effect of the concentration was negligible with an increase from 0.8 to 1.1 wt% [96].

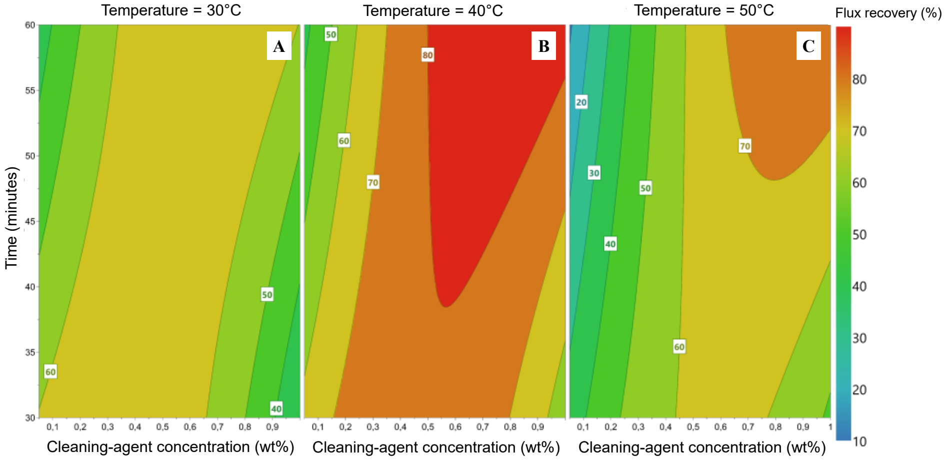

Figure 23: 4D contour plots showing time vs. cleaning-agent concentration at (A) 30ºC, (B) 40ºC, and (C) 50ºC.

Overall, it was concluded that the most optimal conditions for obtaining a flux recovery of greater than 80% are a temperature of 34 – 49ºC, a cleaning time of more than 40 minutes, and a cleaning-agent concentration of 0.5 – 1 wt%.

To obtain an optimised set of parameters using the developed model, the optimiser function in MODDE was used. The model predicted a maximum flux recovery of 88% for a temperature of 40ºC, cleaning time of 60 minutes, and cleaning-agent concentration of 0.8 wt%. When validating the prediction of the model experimentally, i.e. cleaning the membranes under these conditions, a flux recovery of 80% was observed.

3.5. Characterisation of membrane surface and fouling layer

In order to tailor membrane cleaning to a specific process, the types of foulants and their interactions with the membrane surface needed to be studied. For that purpose, the surface of the NF090801 membrane and fouling layer that formed after it had filtered KBL UF permeate were characterised using multiple techniques. Inorganic foulants, such as salts, and organic foulants, such as lignin and hemicelluloses, were analysed. SEM-EDS analysis was used to study the membrane surface and identify the (mostly inorganic) foulants found on membranes that had been conditioned with Ultrasil 110; fouled with KBL UF permeate; and cleaned using the optimised cleaning procedure (**Paper III**). QCM-D was used to analyse the adsorption and desorption behaviour, as well as the layer that the organic foulants formed on a model membrane surface (**Paper IV**).

This section is divided into sub-sections that discuss the conditioned, fouled, and cleaned NF090801 membrane and model surfaces separately.

3.5.1. Characterisation of the conditioned membrane and the model membrane surface

An NF090801 membrane was conditioned with 1 wt% Ultrasil 110 at 50ºC for 60 minutes. SEM showed that the conditioned membrane had a smooth surface, with the exception of a very small quantity of small particles or contaminants (indicated by red circles in Figure 24). EDS analysis showed several elements on the membrane surface, including sodium (Na), magnesium (Mg), sulphur (S), carbon (C), and oxygen (O). These elements can be linked to the composition of the membrane surface itself, which consists of an extremely crosslinked thin-film composite layer, as well as to the conditioning of the membrane. The peaks observed for gold (Au) and palladium (Pd) are related to the sample-preparation process.

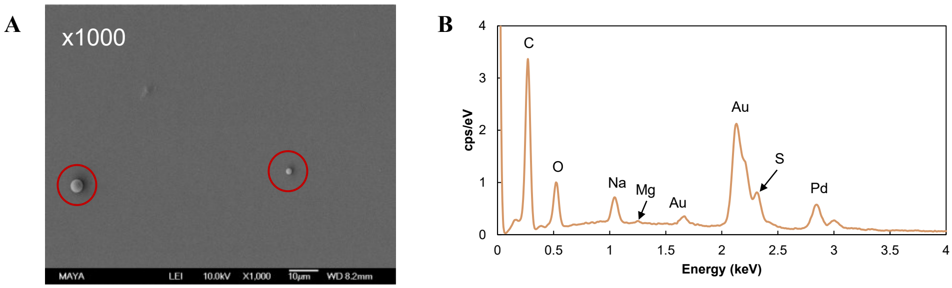

Figure 24: (A) SEM image and (B) EDS spectra of the conditioned NF090801 membrane.

For the QCM-D analysis, the polymer used to manufacture the NF090801 membrane was drop-casted on a quartz sensor in order to model a membrane, which was then characterised using AFM and CA (Figure 25). The model membrane surface exhibited a homogeneous distribution of the polymer on the surface, with a low roughness value of 0.71 ± 0.26 nm and narrow height distribution. The contact angle was 23.6°, which indicated that the surface of the model membrane was hydrophilic.

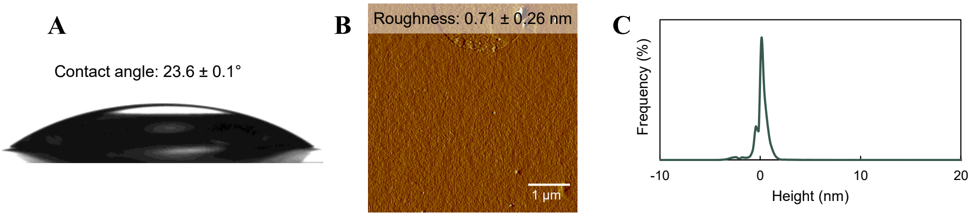

Figure 25: Characteristics of the NF090801 model membrane, which was coated on quartz sensors. Depicted are (A) the contact angle of the model membrane surface, (B) the surface roughness and an AFM image of the surface, and (C) the height distrubution as a histogram.

3.5.2. Characterisation of the fouled membrane and analysis of the fouling layer

An NF090801 membrane was fouled using KBL UF permeate. The SEM images showed several particles scattered on the membrane surface, but no distinct fouling layer. The scattered particles on the surface that were seen at a magnification of x1000 appeared to be deposited salts when viewed at a magnification of x10,000 (red ellipse in Figure 26). The EDS analysis indicated the presence of sodium, magnesium, sulphur, and potassium (K), which could all contribute to the salt formation that can be seen on the membrane surface. The sodium signal was higher on the fouled membrane compared to the conditioned membrane, indicating that it may have been the main inorganic foulant. Carbon and oxygen were also observed, but it is difficult to pinpoint their origin, as it could be from the membrane surface composition or from organic foulants, such as lignin and hemicelluloses.

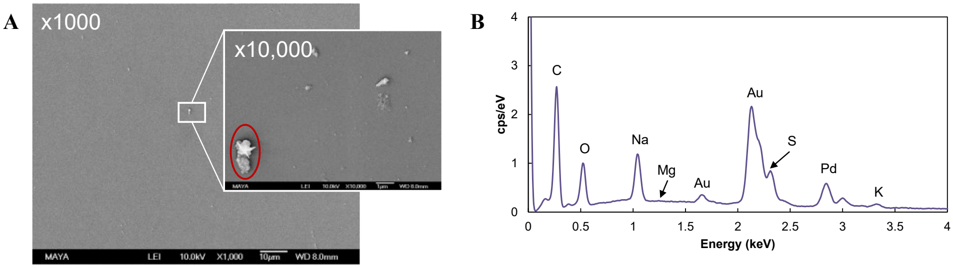

Figure 26: (A) SEM image and (B) EDS spectra of the fouled NF090801 membrane.

Adsorption and desorption of fouling solutions on the model membrane surface

QCM-D was performed at 50°C to investigate the interactions between the foulants in the KBL UF permeate and the model membrane surface (characterised in Section 3.5.1.). Three fouling solutions were used for this purpose: KBL UF permeate, lignin dissolved in NaOH, and hemicelluloses dissolved in NaOH. The lignin and hemicelluloses used for the model solutions were extracted from KBL UF permeate. The adsorption and desorption characteristics of the solutions were detected as variations in the frequency, f (associated with the amount of mass on the surface), and dissipation, D (associated with the softness or rigidity of the fouling layer). A lower frequency indicates that a higher mass was adsorbed on the surface. A higher dissipation indicates a softer layer, whereas a lower dissipation indicates a more rigid layer [45].

The coated sensors were first conditioned with an NaOH solution to establish a baseline (NaOH conditioning phase). The fouling solutions were then introduced to the system in order to study the adsorption of the foulants (fouling phase). Finally, the fouling solutions were rinsed away using NaOH solution in order to study the desorption of the foulants (NaOH rinsing phase).

The frequency decreased immediately when each of the three fouling solutions was introduced to the system (Figure 27A). However, the frequency decreased to -200 Hz when the KBL UF permeate was introduced; to -100 Hz when the lignin was introduced; and to -50 Hz when the hemicelluloses were introduced. This indicates that more of the mass of the components in the KBL UF permeate became attached to the model membrane surface than was the case for the components of the lignin or hemicelluloses solutions individually. The KBL UF permeate contained lignin, hemicelluloses and inorganics, such as salts. The frequency changes indicate that when lignin, hemicelluloses, and salts are all together in solution, all are more prone to becoming attached to the membrane surface. The different components may form complexes or agglomerate with one another, causing them to easily and rapidly become attached to the surface.

When the model membrane surface that had been fouled with KBL UF permeate was rinsed with NaOH solution, the frequency did not return to the initial value, meaning that some components were still attached to the surface. In contrast, when lignin and hemicelluloses were rinsed with NaOH solution, the frequency returned to its initial value in both cases. This implies that that some or most of the mass was rinsed away from the model membrane surface.

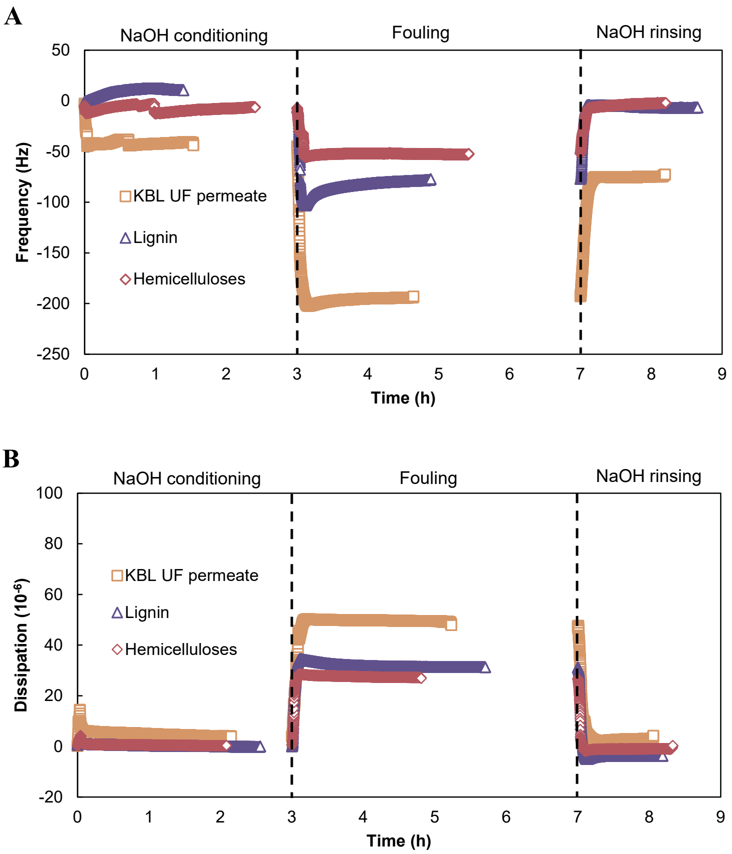

Figure 27: (A) Frequency changes and (B) dissipation changes over time for KBL UF permeate, lignin, and hemicelluloses at 50°C. The data have been adjusted such that the initiation of the NaOH conditioning, fouling, and NaOH rinsing phases are at t = 0 h, t = 3 h, and t = 7 h, respectively.

KBL UF permeate caused the largest change in dissipation, followed by lignin then hemicelluloses (Figure 27B). This means that KBL UF permeate created a softer layer compared to the other two solutions. The dissipation returned to the initial value following rinsing with NaOH for all three solutions. This behaviour can be correlated to the rigidity or softness of the layers, which will be discussed in the next sub-section.

Mass and structure of the fouling layers

Using QCM-D, the adsorbed mass on the model membrane surface was estimated before and after rinsing (Table 9). In addition, the ΔD/Δf ratio, which provides information on the rigidity of the fouling layer, was calculated using the QCM-D data (Figure 28). The adsorbed mass was estimated using the QCM-D software by assuming the density of the fouling solutions to be 996 g/L, and the density for the adsorbed fouling layers to be 1050 g/L (based on the density for hydrated sugar). A lower ΔD/Δf ratio indicates a higher rigidity and density of the layer, whereas a higher value represents a viscoelastic and dissipative layer [97].

Table 9: Adsorbed mass before and after rinsing, and percentage of the total adsobed mass of the three fouling solutions.

Fouling solution	Adsorbed mass before NaOH rinsing (mg/m^2)	Adsorbed mass after NaOH rinsing (mg/m^2)	Mass remaining on the surface (% total adsorbed mass)
KBL UF permeate	554.3 ± 155.3	292.3 ± 203.4	52.7
Lignin	369.6 ± 163.0	104.1 ± 15.4	28.2
Hemicelluloses	177.9 ± 81.5	105.9 ± 13.2	59.5

Large deviations occurred for the adsorbed mass before and after rinsing with NaOH for KBL UF permeate. This suggests that the mass of the solution was not adsorbed uniformly on the model membrane surface. The layer created by the KBL UF permeate seemed to be soft, based on the ΔD/Δf ratio, which is in line with the dissipation results. Following NaOH rinsing the layer became less soft, and 52.7% of the mass remained on the surface.

For lignin, the significant deviation suggests that the mass was not adsorbed uniformly. However, most of the lignin mass was removed by NaOH rinsing and, similar to the KBL UF permeate, the layer became more rigid after rinsing.

Hemicelluloses seemed to be more resistant to NaOH rinsing than lignin and KBL UF permeate, as 59.5% of the hemicelluloses mass remained on the surface after rinsing. This may have been due to the rigidity of the layer, as the hemicelluloses solution created the most rigid layer of the three fouling solutions. However, following NaOH rinsing, the large standard deviation in the ΔD/Δf ratio for the hemicelluloses made it difficult to determine whether the hemicelluloses layer became soft or remained rigid.

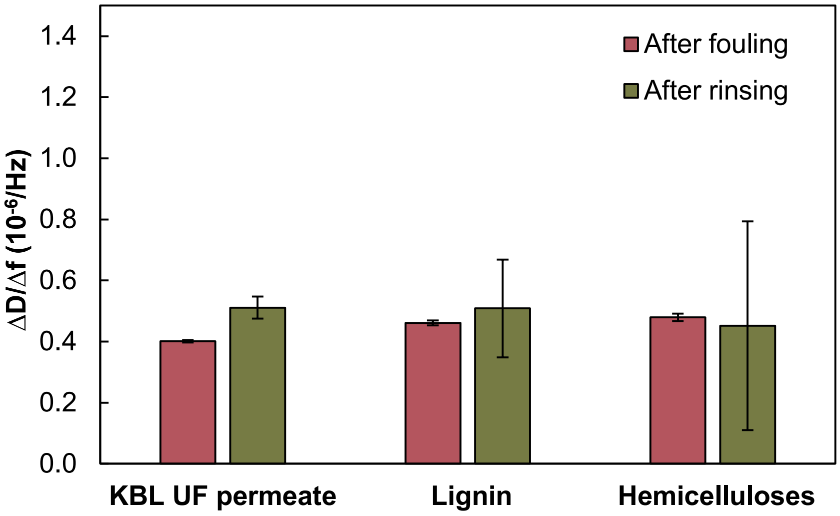

Figure 28: ΔD/Δf ratios after fouling and after NaOH rinsing for KBL UF permeate, lignin, and hemicelluloses at 50°C.

3.5.3. Characterisation of the cleaned membrane

After being fouled, an NF090801 membrane was cleaned using the optimal cleaning parameters discussed in Section 3.4: 60 minutes cleaning time, 40°C, and an Ultrasil 110 concentration of 0.8 wt%. The membrane was then characterised using SEM-EDS.

The cleaned membrane showed a relatively smooth surface, besides some small particles that were visible at a magnification of x250. One of these (marked with a red circle in Figure 29) appeared to be a salt particle, similar to those observed on the fouled membrane (Figure 26). The main difference between the particles observed on the fouled and cleaned membrane surfaces was that the particles on the cleaned membrane seemed to have openings; these may have been caused by the cleaning, with part of the particle being washed away. The flux recovery obtained during the experimental validation of the optimised cleaning method (Section 3.4.2.) could be explained by the presence of these particles (which may have been partially washed away by cleaning) on an otherwise smooth and clean membrane surface. Therefore, foulants were still present, explaining why a flux recovery exceeding 80% was not obtained with the optimised cleaning. Moreover, the EDS spectra showed that the sodium signal returned to almost the same level as the conditioned membrane, corroborating what was observed using SEM and the results of the experimental validation of the cleaning model.

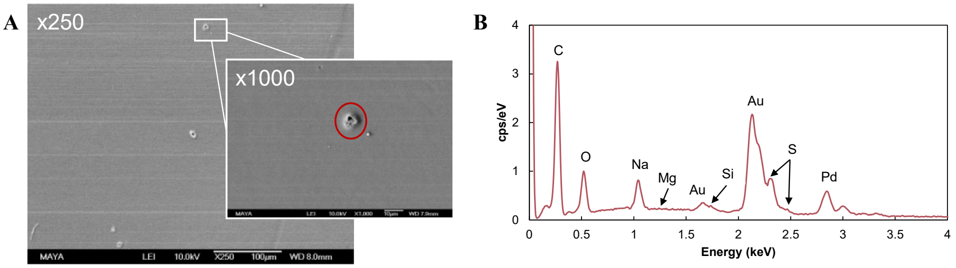

Figure 29: (A) SEM image and (B) EDS spectra of the cleaned NF090801 membrane.

3.5.4. Implications for cleaning membranes fouled with kraft black liquor ultrafiltration permeate

KBL UF permeate contains both organic and inorganic foulants, both of which were observed on the membrane surface and model membrane surface when fouled. The QCM-D experiments indicated that the KBL UF permeate did not create a uniform layer on the model membrane surface, which was confirmed by the SEM analysis, where no clear fouling layer was observed.

During the parametric and concentration studies performed at laboratory and pilot scales, rinsing with an NaOH solution was performed following KBL UF permeate filtration in order to avoid lignin precipitation on the membranes. This step may have helped to remove some of the foulants from the membrane surface, as NaOH has previously been used as a standalone cleaning agent [96,98]. However, as is indicated by the PWF measurements, chemical cleaning was necessary in order to recover the flux. Thus, NaOH rinsing was not sufficient to remove all of the fouling caused by KBL UF permeate on the membranes.

The QCM-D experiments with lignin showed that the NaOH rinsing removed more than 70% of the absorbed lignin mass on the model membrane surface. However, this was not the case when the layers formed by the hemicelluloses and KBL UF permeate were rinsed, as more than half of the mass of both stayed on the surface. Rudolph et al. reported a rigid layer formed by hemicelluloses on a polysulfone model membrane, and that 60% of the mass stayed on the surface following rinsing with MilliQ water [97]. This can indicate that, generally, hemicelluloses cause the formation of a rigid layer on a membrane surface and that rinsing with water or NaOH solution is not enough to remove the layer. The hemicelluloses in the KBL UF permeate might be one of the causes that rinsing with NaOH solution does not fully remove the adsorbed mass on the coated sensor.

The information gathered with the SEM-EDS analysis and the QCM-D experiments can be used to tailor the chemical cleaning to remove the components from KBL

UF permeate, such as hemicelluloses and sodium salts, that adsorb the most on the membrane surface and cause fouling.

3.6. Techno-economic evaluation

Two techno-economic evaluations were performed in order to evaluate different aspects of the NF of KBL UF permeate. The first evaluated the viability of implementing NF after UF in a pulp and paper mill, and how membrane filtration streams could be used within the mill (**Paper II**). The second compared the cleaning costs of a standard cleaning procedure to the optimised one presented in Section 3.4 (**Paper III**).

For both techno-economic evaluations, the calculations were based on an NF membrane plant receiving a flow of 112 t/h of KBL UF permeate, and producing 89 t/h of permeate (Figure 30). Before the NF step, there is a UF membrane plant that takes 140 t/h KBL directly from the mill, equal to 15% of the total amount of KBL produced in the pulp mill. The UF step concentrates the KBL up to a VR of 80%. This step was not considered in the techno-economic evaluations.

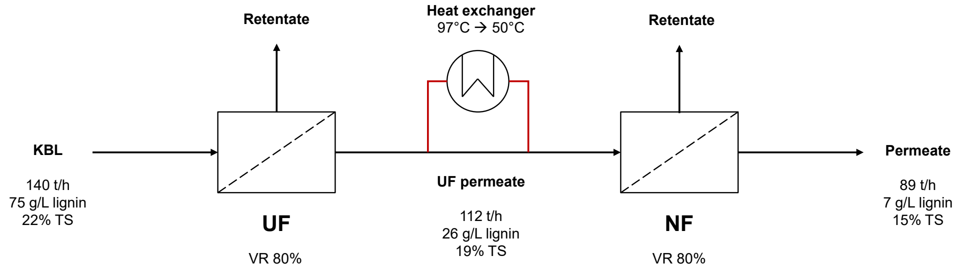

Figure 30: Process diagram of the UF and NF steps used to design the membrane filtration plant and estimate the costs.

The capital expenses (CapEx) were the costs of the installation of the membrane plant and the initial set of membranes. The operating expenses (OpEx) were the costs of maintenance and labour, membrane replacement and cleaning, and electricity. For each techno-economic evaluation, CapEx and OpEx were calculated using experimental parameters, and data from manufacturers. Although the NF plant treated the same amount of KBL UF permeate in the two evaluations, the plant design, and the CapEx and OpEx differed due to the different assumptions made in each techno-economic evaluation.

3.6.1. Economic feasibility of implementing a nanofiltration membrane plant

Four different scenarios were considered in the first techno-economic evaluation (Figure 31). These scenarios considered the uses of the membrane filtration streams: for lignin extraction, reuse within the mill, or being returned to the evaporator plant. Detailed explanations of the NF membrane plant design and the CapEx and OpEx that were used to calculate the impacts of each scenario can be found in **Paper II**.

The scenarios and uses of the UF and NF streams were:

- **Scenario 1**: Reference kraft pulp mill, without lignin extraction.
- **Scenario 2**: Kraft pulp mill with a UF step before the evaporators. The UF retentate is used for lignin extraction, and the UF permeate is returned to the evaporators.
- **Scenario 3**: Kraft pulp mill with lignin extraction using combined UF-NF. The UF retentate is used for lignin extraction, while the UF permeate goes into the NF step. The NF retentate provides extra lignin recovery, while the NF permeate is sent to the smelt dissolving tank.
- **Scenario 4**: Kraft pulp mill with combined UF-NF. The UF retentate is used for lignin extraction, while the UF permeate goes into the NF step for dewatering. The NF permeate is sent to the smelt dissolving tank and the NF retentate is sent to the evaporators.

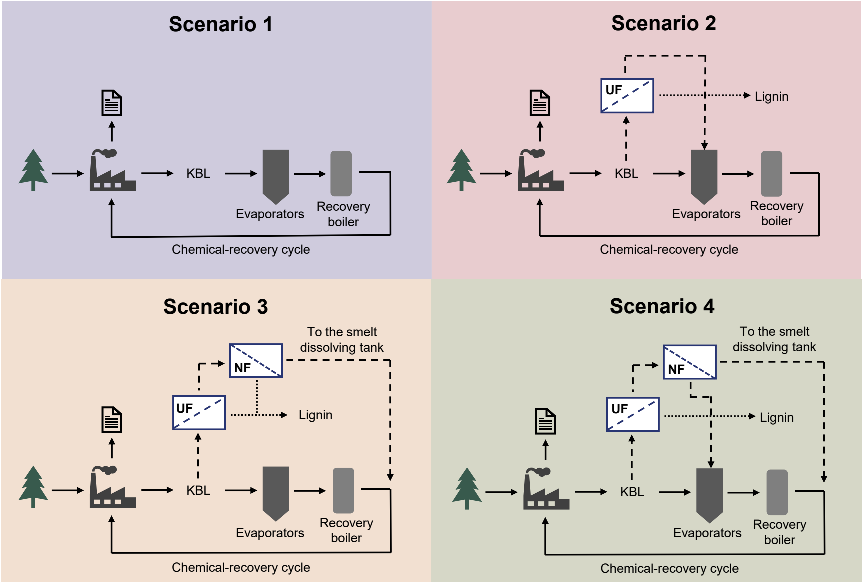

Figure 31: The four scenarios that were considered in the techno-economic evaluation.

It is important to note that the NF permeate contains 7 g/L of lignin (Figure 30). Ideally, however, NF permeate that is sent to a smelt dissolving tank should have no lignin. Therefore, in order to simplify the calculations for the purposes of the techno-economic evaluation, it was assumed that the NF separation is perfect, and that the permeate does not contain lignin.

The impact of lignin recovery was considered regarding energy production in the recovery boiler, the steam consumption of the evaporators, and electrical-power generation (Table 10). The reference mill was based on the FRAM model mill for bleached kraft pulp [99]. The model mill was adjusted for production of 3000 ADt/d with 70% softwood and 30% hardwood. The electricity cost was 0.035 €/kWh, which is the average of the spot price in the north of Sweden between 2018 and 2021.

Scenario 1 is the reference scenario, meaning that no lignin is extracted. Comparing the three other scenarios to the reference scenario, the largest impact of lignin recovery is the reduced energy production of the recovery boiler. This is because less lignin is burned, and it was assumed that pulp production would not increase.

In Scenario 2, the addition of the UF permeate to the evaporators increases their energy demand slightly, from 109 to 111 MW. In contrast, in Scenarios 3 and 4, the NF step slightly reduces the energy demand of the evaporators. The steam consumption of the evaporators directly affects the amount of electricity generated by the turbine; the less steam the evaporators consume, the more electricity is generated.

Scenarios 2, 3, and 4 have lower electrical-power generation compared to Scenario 1 because less lignin is available as fuel. Scenarios 2 and 4 are very similar since they both recover the same amount of lignin, and differ only in terms of the steam consumption of the evaporators. In Scenario 4 the evaporators require less energy due to the NF process. This translates into a net increase in electrical power generation of 19.4 GWh/year in Scenario 4 as compared to Scenario 2. This electrical power could then be sold, resulting in a revenue of 680,000 €/year. Since this value exceeds the OpEx of the membrane plant, which is 296,200 €/year, the payback time of the membrane plant in Scenario 4 is 2.2 years.

Table 10: Impact of lignin recovery on energy production and consumption in the mill.

	Scenario 1	Scenario 2	Scenario 3	Scenario 4
Lignin recovered (t/h)	0	7.0	9.6	7.0
Energy generation in recovery boiler (MW)	571	529	513	529
Steam consumption of evaporators (MW)	109	111	104	103
Electrical power generation (MW)	143	126	122	129

3.6.2. Costs of membrane cleaning

In this section, the second techno-economic analysis is presented; this compared the costs of a standard and an optimised membrane cleaning in a model NF membrane plant. Therefore, a model NF membrane plant was designed (Figure 32) to be able to calculate the CapEx and OpEx. The plant consisted of three loops, two of them with 10 pressure vessels and one with 8 pressure vessels. Each pressure vessel contained four spiral wound membranes. The plant was designed to have one feed pump and three recirculation pumps to ensure a feed flow of 112 m^3/h, a retentate flow of 22 m^3/h and a permeate flow of 90 m^3/h. The detailed calculations for the design of the model NF membrane plant can be found in **Paper III**.

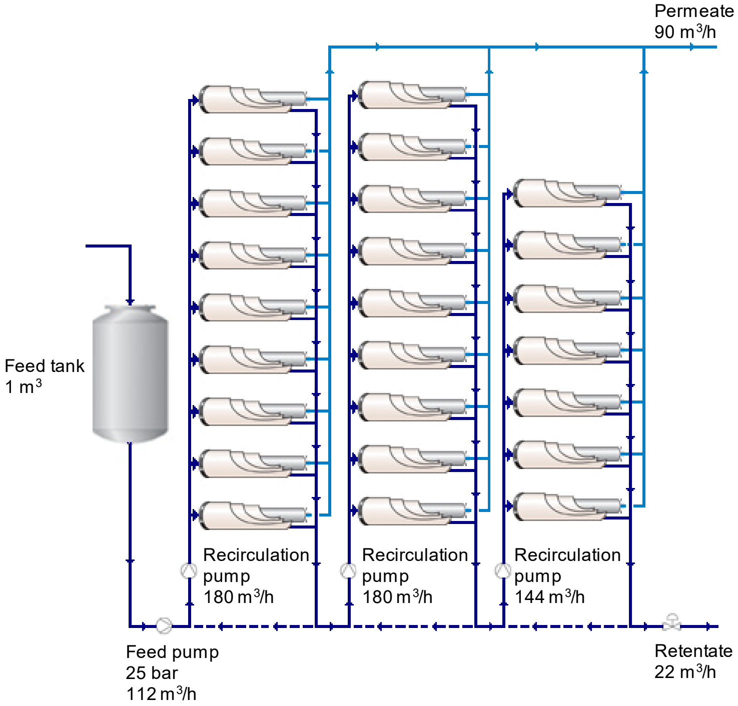

Figure 32: NF membrane plant design for the treatment of KBL UF permeate.

It was assumed for both the standard and optimised cleaning scenario that the membranes were cleaned for 1 h every two days. In the standard cleaning scenario, the membranes were cleaned at 50°C and with a cleaning-agent concentration of 1 wt%. In the optimised cleaning scenario, the membranes were cleaned at 40°C and with a cleaning-agent concentration of 0.8 wt% (the optimised cleaning method presented in Section 3.4.).

The cost of water was taken into consideration in the techno-economic analysis. During the experimental part reported in **Paper III**, it was noted that a lower cleaning-agent concentration required less water when rinsing the membrane equipment. It was therefore assumed that the rinsing volume for the standard cleaning would be 3.5 times the internal volume of the NF membrane plant, while for the optimised cleaning it would be 3 times the internal volume of the NF membrane plant. Moreover, it was assumed that, from the total operating time, 7832 h were dedicated to production, i.e. NF of KBL UF permeate, and 168 h to membrane cleaning. The remaining parameters used for the calculations of the costs are given in **Paper III**.

The difference between the two scenarios lies in the membrane-cleaning costs, which are part of the OpEx. These consist of the cost of the cleaning agent and electricity (for the pumps), and water and heating (Table 11). Overall, using the optimised cleaning method instead of the standard one would save 16% of the membrane-cleaning costs, or about 768 € in OpEx per year.

Table 11: Membrane-cleaning costs for the two scenarios considered, and the savings that could be achieved by using the optimised cleaning process (€/year).

Membrane-cleaning costs	Standard cleaning	Optimised cleaning	Savings
Cleaning agent	1670.00	1336.00	334.00
Electricity	232.91	232.91	0.00
Water usage	2726.12	2360.53	365.59
Heating	273.31	204.98	68.33
Total (€/year)	4902.35	4134.43	767.92

The electricity costs are the same for both scenarios, as they are the cost of pump operation during the cleaning. The same cleaning time, TMP, and CFV were assumed in both scenarios. Further savings could be made if the TMP and time could be reduced, although it would be important for these reductions to not compromise flux recovery. The investigation of the optimised cleaning procedure showed that 60 minutes was the optimal duration for removing most of the foulants and obtaining a flux recovery of 80%. Reducing the cleaning time could lead to failure to remove sufficient amounts of fouling at the membrane surface, potentially compromising the filtration capacity of the membranes later.

4. Concluding remarks

The research presented in this thesis investigated the implementation of a NF step in an integrated two-step UF-NF process for concentrating KBL in a pulp and paper mill. The goal of the NF filtration step is to concentrate KBL UF permeate for the purposes of lignin recovery and obtaining a permeate that can be reused in the mill. The performance of a chosen membrane (NF090801) was studied, and the standard method of cleaning membranes in this context was optimised.

The first step was to choose an adequate membrane for the NF that could further concentrate the UF permeate. Several commercial NF membranes were tested at laboratory scale, and one (NF090801) was chosen based on its flux and lignin retention. The selected membrane was tested at pilot scale under two different operating conditions. When operated at 50ºC and 25 bar, the membrane had an average lignin retention of 82%; at 70ºC and 15 bar, it had an average lignin retention of 77%. Analysis suggested a change in membrane morphology and damage to the membrane surface as a result of operating at 70ºC. It was concluded that 50ºC and 25 bar were the adequate operating conditions for the chosen membrane at pilot scale.

The experimental data generated at pilot scale, with the membrane operated at 50ºC and 25 bar, was used to evaluate the membrane filtration streams produced in an NF membrane plant in a techno-economic analysis. It was determined that it is more economically beneficial to use the NF step for dewatering the UF permeate than for additional lignin extraction.

After the investigation and selection of a membrane and operating conditions for the NF step, the cleaning procedure was optimised using RSM. The model found that cleaning at a temperature of 40ºC with 0.8 wt% Ultrasil 110 for 60 minutes achieved a flux recovery of 88%. When the cleaning conditions were validated experimentally, a flux recovery of 80% was obtained. Therefore, a model that could successfully predict flux recovery given the cleaning parameters was developed. The techno-economic evaluation showed that the optimised cleaning method can reduce membrane-cleaning costs by 16%.

Membrane fouling was studied using multiple techniques. SEM imaging showed that no distinct fouling layer was created by the KBL UF permeate, and that instead it appeared that particles were scattered over the surface. EDS analysis showed that sodium was the main inorganic foulant, and that the optimised cleaning method successfully removed this from the membrane surface. A membrane surface was modelled on a quartz sensor, and characterised using AFM and CA. The model membrane surfaces were used in QCM-D studies to observe the adsorption and desorption behaviour of KBL UF permeate, lignin, and hemicelluloses. It was shown that the components of KBL UF permeate, such as lignin, hemicelluloses, and salts, form complexes that adsorb faster and more permanently to the model membrane surface than lignin does on its own. Rinsing with an NaOH solution did not fully remove the fouling layer that resulted from filtering KBL UF permeate and hemicelluloses, indicating that hemicelluloses might be the cause that the KBL UF permeate adsorbed more permanently on the model membrane surface.

In summary, the work presented in this thesis demonstrates that it is possible to implement a UF-NF membrane plant in a pulp and paper mill. The UF step achieves lignin extraction, and the NF step the dewatering of the UF permeate, allowing the streams produced by NF to be reused in the mill. The NF step decreases the energy demand of the evaporators, creating a net increase in electrical-power generation. Moreover, the optimised cleaning method reduces membrane-cleaning costs and improves flux recovery. The study of membrane fouling provided insights regarding what are the main foulants and how they interact with the membrane surface. Although this thesis focused on the development of one membrane-filtration step, it proves that research and development of separation processes can be successful, and that, step by step, more biorefinery processes can be implemented in pulp and paper mills.

5. Future perspectives

The research presented in this thesis has proven that it is feasible to have an NF filtration step after a UF step in a pulp and paper mill. However, there are several aspects that would benefit from further research and development.

When the NF090801 membrane was operated at 70ºC at pilot scale, the data suggests that its morphology changed and the surface was damaged. It was concluded that this temperature was too high for the membrane. Testing other available commercial membranes that can withstand high temperatures and high pH would be one way of overcoming the shortcomings of the NF090801 membrane. For example, other NF ceramic membranes could be tested when they become commercially available. Another option would be to test non-commercial membranes that are being developed by other researchers. For example, polyethersulphone-supported graphene oxide membranes have been shown to operate at high pH and relatively high temperatures when filtering KBL [25,26]. These membrane could be a promising solution for filtering KBL UF permeate but further research efforts are required to produce them on larger-scale.

RSM proved to be a valuable tool for optimising membrane cleaning. However, the model that was developed was specific to the process and membrane that were being investigated. Therefore, it would be useful to develop a larger model that could be applied to more than one process and membrane and include other operating parameters, such as TMP and CFV. To do this, more experimental data would need to be collected, and the range of the model more broadly defined. For example, the model could optimise the cleaning parameters for membrane processes applied to pulp and paper mill effluents. Machine learning could be used to handle the large amounts of data collected and the resulting model. In other fields that utilise membrane technology, such as water and wastewater treatment, artificial intelligence and machine learning have been beneficially applied when developing models to control fouling [100] and optimise filtration performance [101]. These tools could therefore be applied to the development of a model for the optimisation of cleaning in membrane processes for pulp and paper mill effluents.

The optimised cleaning procedure recovered 80% of the flux and removed the majority of the foulants. As shown by SEM-EDS analysis, some foulants remained on the membrane following the optimised alkaline chemical cleaning, however. To remove the remaining foulants, an additional cleaning step that uses an acidic cleaning agent could be added to the cleaning procedure, since some of the foulants that were observed were inorganic. This combination of alkaline and acidic cleaning should be tested to ascertain whether the additional cleaning step increases or decreases the final flux recovery.

The QCM-D experiments showed that some interactions occurred between the foulants contained in the KBL UF permeate (lignin, hemicelluloses, and salts), but it is unclear how these interactions work. Further QCM-D experiments combined with other *in-situ* fouling techniques, such as ellipsometry or liquid-state AFM, could be performed in order to better understand the interactions between foulants, as an understanding of fouling is fundamental to tailoring cleaning procedures to specific membrane-filtration processes.

References

[1] K. Calvin, D. Dasgupta, G. Krinner, A. Mukherji, P.W. Thorne, C. Trisos, J. Romero, P. Aldunce, K. Barrett, G. Blanco, W.W.L. Cheung, S. Connors, F. Denton, A. Diongue-Niang, D. Dodman, M. Garschagen, O. Geden, B. Hayward, C. Jones, F. Jotzo, T. Krug, R. Lasco, Y.-Y. Lee, V. Masson-Delmotte, M. Meinshausen, K. Mintenbeck, A. Mokssit, F.E.L. Otto, M. Pathak, A. Pirani, E. Poloczanska, H.-O. Pörtner, A. Revi, D.C. Roberts, J. Roy, A.C. Ruane, J. Skea, P.R. Shukla, R. Slade, A. Slangen, Y. Sokona, A.A. Sörensson, M. Tignor, D. van Vuuren, Y.-M. Wei, H. Winkler, P. Zhai, Z. Zommers, J.-C. Hourcade, F.X. Johnson, S. Pachauri, N.P. Simpson, C. Singh, A. Thomas, E. Totin, A. Alegría, K. Armour, B. Bednar-Friedl, K. Blok, G. Cissé, F. Dentener, S. Eriksen, E. Fischer, G. Garner, C. Guivarch, M. Haasnoot, G. Hansen, M. Hauser, E. Hawkins, T. Hermans, R. Kopp, N. Leprince-Ringuet, J. Lewis, D. Ley, C. Ludden, L. Niamir, Z. Nicholls, S. Some, S. Szopa, B. Trewin, K.-I. van der Wijst, G. Winter, M. Witting, A. Birt, M. Ha, IPCC, 2023: Climate Change 2023: Synthesis Report. Contribution of Working Groups I, II and III to the Sixth Assessment Report of the Intergovernmental Panel on Climate Change [Core Writing Team, H. Lee and J. Romero (eds.)]. IPCC, Geneva, Switzerland., 2023. https://doi.org/10.59327/IPCC/AR6-9789291691647.

[2] B. Kamm, M. Kamm, Principles of biorefineries, Applied Microbiology Biotechnology 64 (2004) 137–145. https://doi.org/10.1007/s00253-003-1537-7.

[3] B. Annevelink, L. Garcia Chavez, R. van Ree, I. Vural Gursel, G. Bell, M. Mandl, J. Lindorfer, F. Hesser, X. Hilz, T. Stern, S. Mussatto, H. Stichnothe, J. Leahy, I. De Bari, V. Motola, A. Giuliano, E. de Jong, J. Mossberg, M. Shmorhun, Global biorefinery status report 2022, 2022.

[4] H.-J. Huang, S. Ramaswamy, U.W. Tschirner, B.V. Ramarao, A review of separation technologies in current and future biorefineries, Sep Purif Technol 62 (2008) 1–21. https://doi.org/10.1016/j.seppur.2007.12.011.

[5] H. Strathmann, Synthetic Membranes and Their Preparation, in: Synthetic Membranes: Science, Engineering and Applications, Springer Netherlands, Dordrecht, 1986: pp. 1–37. https://doi.org/10.1007/978-94-009-4712-2_1.

[6] F. Lipnizki, J. Thuvander, G. Rudolph, Membrane processes and applications for biorefineries, in: Current Trends and Future Developments on (Bio-) Membranes, Elsevier, 2020: pp. 283–301. https://doi.org/10.1016/B978-0-12-816778-6.00013-8.

[7] Y. He, D.M. Bagley, K.T. Leung, S.N. Liss, B.-Q. Liao, Recent advances in membrane technologies for biorefining and bioenergy production, Biotechnol Adv 30 (2012) 817–858. https://doi.org/10.1016/j.biotechadv.2012.01.015.

[8] A.-S. Jönsson, R. Wimmerstedt, The application of membrane technology in the pulp and paper industry, Desalination 53 (1985) 181–196. https://doi.org/10.1016/0011-9164(85)85060-8.

[9] U. Haagensen, Applications in the Pulp and Paper Industry, 1982.

[10] S. Cortiñas, S. Luque, J.R. Álvarez, J. Canaval, J. Romero, Microfiltration of kraft black liquors for the removal of colloidal suspended matter (pitch), Desalination 147 (2002) 49–54. https://doi.org/10.1016/S0011-9164(02)00575-1.

[11] G. Liu, Y. Liu, J. Ni, H. Shi, Y. Qian, Treatability of kraft spent liquor by microfiltration and ultrafiltration, Desalination 160 (2004) 131–141. https://doi.org/10.1016/S0011-9164(04)90003-3.

[12] T.K. Fagbemigun, M.A. Azeez, J. Odermatt, Ultrafiltration of Industrial Hardwood Kraft Black Liquor with Regenerated Cellulose Membrane, IOSR Journal of Applied Chemistry (IOSR-JAC 15 (2022) 22–39. https://doi.org/10.9790/5736-1501012239.

[13] A. Toledano, A. García, I. Mondragon, J. Labidi, Lignin separation and fractionation by ultrafiltration, Sep Purif Technol 71 (2010) 38–43. https://doi.org/10.1016/j.seppur.2009.10.024.

[14] P. Kekana, B. Sithole, D. Ramjugernath, Stirred cell ultrafiltration of lignin from black liquor generated from South African kraft mills, S Afr J Sci Volume 112 (2016) 1–7. https://doi.org/10.17159/sajs.2016/20150280.

[15] C.A.E. Costa, P.C.R. Pinto, A.E. Rodrigues, Lignin fractionation from E. Globulus kraft liquor by ultrafiltration in a three stage membrane sequence, Sep Purif Technol 192 (2018) 140–151. https://doi.org/10.1016/j.seppur.2017.09.066.

[16] O. Wallberg, A.S. Jönsson, R. Wimmerstedt, Fractionation and concentration of kraft black liquor lignin with ultrafiltration, Desalination 154 (2003) 187–199. https://doi.org/10.1016/S0011-9164(03)80019-X.

[17] M. Mänttäri, J. Lahti, H. Hatakka, M. Louhi-Kultanen, M. Kallioinen, Separation phenomena in UF and NF in the recovery of organic acids from kraft black liquor, J Memb Sci 490 (2015) 84–91. https://doi.org/10.1016/j.memsci.2015.04.048.

[18] M. Sharma, P. Alves, L.M. Gando-Ferreira, Lignin Recovery from Black Liquor Using Integrated UF/NF Processes and Economic Analysis, Membranes (Basel) 13 (2023). https://doi.org/10.3390/membranes13020237.

[19] A. Arkell, J. Olsson, O. Wallberg, Process performance in lignin separation from softwood black liquor by membrane filtration, Chemical Engineering Research and Design 92 (2014) 1792–1800. https://doi.org/10.1016/j.cherd.2013.12.018.

[20] A. Keyoumu, R. Sjödahl, G. Henriksson, M. Ek, G. Gellerstedt, M.E. Lindström, Continuous nano- and ultra-filtration of kraft pulping black liquor with ceramic filters: A method for lowering the load on the recovery boiler while generating valuable side-products, Ind Crops Prod 20 (2004) 143–150. https://doi.org/10.1016/j.indcrop.2004.04.017.

[21] A.S. Jönsson, A.K. Nordin, O. Wallberg, Concentration and purification of lignin in hardwood kraft pulping liquor by ultrafiltration and nanofiltration, Chemical Engineering Research and Design 86 (2008) 1271–1280. https://doi.org/10.1016/j.cherd.2008.06.003.

[22] A.S. Jönsson, O. Wallberg, Cost estimates of kraft lignin recovery by ultrafiltration, Desalination 237 (2009) 254–267. https://doi.org/10.1016/j.desal.2007.11.061.

[23] Z. Wang, C. Ma, A. Shen, A. Berchenko, S.A. Sinquefield, S. Nair, Kraft black liquor concentration with graphene oxide membranes: Process simulations and technoeconomic analysis, J Adv Manuf Process 3 (2021). https://doi.org/10.1002/amp2.10104.

[24] O.J. Valderrama, K.L. Zedda, S. Velizarov, Membrane filtration opportunities for the treatment of black liquor in the paper and pulp industry, Water (Switzerland) 13 (2021). https://doi.org/10.3390/w13162270.

[25] Z. Wang, C. Ma, S.A. Sinquefield, M.L. Shofner, S. Nair, High-Performance Graphene Oxide Nanofiltration Membranes for Black Liquor Concentration, ACS Sustain Chem Eng 7 (2019) 14915–14923. https://doi.org/10.1021/acssuschemeng.9b03113.

[26] F. Rashidi, N.S. Kevlich, S.A. Sinquefield, M.L. Shofner, S. Nair, Graphene Oxide Membranes in Extreme Operating Environments: Concentration of Kraft Black Liquor by Lignin Retention, ACS Sustain Chem Eng 5 (2017) 1002–1009. https://doi.org/10.1021/acssuschemeng.6b02321.

[27] H.J. Huang, S.R. Ramaswamy, Overview of Biomass Conversion Processes and Separation and Purification Technologies in Biorefineries, in: Separation and Purification Technologies in Biorefineries, wiley, 2013: pp. 3–36. https://doi.org/10.1002/9781118493441.ch1.

[28] G. Rudolph-Schöpping, T. Rissanen, M. Kallionen, F. Lipnizki, Focus on fouling monitoring, Filtration + Separation 56 (2019) 25–27. https://doi.org/10.1016/S0015-1882(20)30106-3.

[29] M. Mulder, Membrane Processes, in: Basic Principles of Membrane Technology, 2nd Edition, Kluwer Academic Publishers, Dordrecht, 1996: pp. 280–415.

[30] M.N. de Pinho, M. Minhalma, Introduction in Membrane Technologies, in: Separation of Functional Molecules in Food by Membrane Technology, Elsevier, 2019: pp. 1–29. https://doi.org/10.1016/B978-0-12-815056-6.00001-2.

[31] B. Van der Bruggen, Microfiltration, ultrafiltration, nanofiltration, reverse osmosis, and forward osmosis, in: Fundamental Modeling of Membrane Systems: Membrane and Process Performance, Elsevier, 2018: pp. 25–70. https://doi.org/10.1016/B978-0-12-813483-2.00002-2.

[32] W.J. Koros, Y.H. Ma, T. Shimidzu, Terminology for membranes and membrane processes (IUPAC Recommendation 1996), J Memb Sci 120 (1996) 149–159. https://doi.org/10.1016/0376-7388(96)82861-4.

[33] Z.F. Cui, Y. Jiang, R.W. Field, Fundamentals of Pressure-Driven Membrane Separation Processes, in: Membrane Technology, Elsevier, 2010: pp. 1–18. https://doi.org/10.1016/B978-1-85617-632-3.00001-X.

[34] A.-S. Jönsson, B. Jönsson, 9. Pure water flux, (n.d.).

[35] A.-S. Jönsson, B. Jönsson, 10. Flux - basic models, (n.d.).

[36] A.-S. Jönsson, B. Jönsson, 11. Critical flux, (n.d.).

[37] P. Aimar, V. Sanchez, A novel approach to transfer-limiting phenomena during ultrafiltration of macromolecules, Industrial & Engineering Chemistry Fundamentals 25 (1986) 789–798. https://doi.org/10.1021/i100024a052.

[38] R.W. Field, D. Wu, J.A. Howell, B.B. Gupta, Critical flux concept for microfiltration fouling, J Memb Sci 100 (1995) 259–272. https://doi.org/10.1016/0376-7388(94)00265-Z.

[39] P. Bacchin, P. Aimar, R. Field, Critical and sustainable fluxes: Theory, experiments and applications, J Memb Sci 281 (2006) 42–69. https://doi.org/10.1016/j.memsci.2006.04.014.

[40] A.-S. Jönsson, B. Jönsson, 5. Retention of large, uncharged molecules, (n.d.).

[41] A. Abdelrasoul, H. Doan, A. Lohi, Fouling in Membrane Filtration and Remediation Methods, in: Mass Transfer - Advances in Sustainable Energy and Environment Oriented Numerical Modeling, InTech, 2013. https://doi.org/10.5772/52370.

[42] M. Mulder, Polarisation phenomena and fouling, in: Basic Principles of Membrane Technology, 2nd edition, Kluwer Academic Publishers, 1996: pp. 416–464.

[43] R. Field, Fundamentals of Fouling, in: Membrane Technology, Wiley, 2010: pp. 1–23. https://doi.org/10.1002/9783527631407.ch1.

[44] G. Rudolph, T. Virtanen, M. Ferrando, C. Güell, F. Lipnizki, M. Kallioinen, A review of in situ real-time monitoring techniques for membrane fouling in the biotechnology, biorefinery and food sectors, J Memb Sci 588 (2019) 117221. https://doi.org/10.1016/j.memsci.2019.117221.

[45] A.D. Easley, T. Ma, C.I. Eneh, J. Yun, R.M. Thakur, J.L. Lutkenhaus, A practical guide to quartz crystal microbalance with dissipation monitoring of thin polymer films, Journal of Polymer Science 60 (2022) 1090–1107. https://doi.org/10.1002/pol.20210324.

[46] M. Edvardsson, S. Svedhem, G. Wang, R. Richter, M. Rodahl, B. Kasemo, QCM-D and Reflectometry Instrument: Applications to Supported Lipid Structures and Their Biomolecular Interactions, Anal Chem 81 (2009) 349–361. https://doi.org/10.1021/ac801523w.

[47] X. Wang, D. Huang, B. Cheng, L. Wang, New insight into the adsorption behaviour of effluent organic matter on organic–inorganic ultrafiltration membranes: a combined QCM-D and AFM study, R Soc Open Sci 5 (2018) 180586. https://doi.org/10.1098/rsos.180586.

[48] G. Rudolph-Schöpping, H. Schagerlöf, A.-S. Jönsson, F. Lipnizki, Comparison of membrane fouling during ultrafiltration with adsorption studied by quartz crystal microbalance with dissipation monitoring (QCM-D), J Memb Sci 672 (2023) 121313. https://doi.org/10.1016/j.memsci.2022.121313.

[49] E.S. Muckley, L. Collins, B.R. Srijanto, I.N. Ivanov, Machine Learning-Enabled Correlation and Modeling of Multimodal Response of Thin Film to Environment on Macro and Nanoscale Using “Lab-on-a-Crystal,” Adv Funct Mater 30 (2020). https://doi.org/10.1002/adfm.201908010.

[50] N. Stein, R. Sharon-Gojman, M.S. Mauter, R. Bernstein, M. Herzberg, Fouling of Reverse Osmosis Membrane with Effluent Organic Matter: Componential Role of Hydrophobicity, ACS ES&T Water 3 (2023) 2491–2501. https://doi.org/10.1021/acsestwater.3c00116.

[51] J.T. Kim, N. Weber, G.H. Shin, Q. Huang, S.X. Liu, The Study of β-Lactoglobulin Adsorption on Polyethersulfone Thin Film Surface Using QCM-D and AFM, J Food Sci 72 (2007). https://doi.org/10.1111/j.1750-3841.2007.00344.x.

[52] S.X. Liu, J.-T. Kim, Application of Kevin—Voigt Model in Quantifying Whey Protein Adsorption on Polyethersulfone Using QCM-D, JALA: Journal of the Association for Laboratory Automation 14 (2009) 213–220. https://doi.org/10.1016/j.jala.2009.01.003.

[53] A. Eskhan, N. AlQasas, D. Johnson, Interaction Mechanisms and Predictions of the Biofouling of Polymer Films: A Combined Atomic Force Microscopy and Quartz Crystal Microbalance with Dissipation Monitoring Study, Langmuir 39 (2023) 6592–6612. https://doi.org/10.1021/acs.langmuir.3c00587.

[54] A. Sweity, W. Ying, M.S. Ali-Shtayeh, F. Yang, A. Bick, G. Oron, M. Herzberg, Relation between EPS adherence, viscoelastic properties, and MBR operation: Biofouling study with QCM-D, Water Res 45 (2011) 6430–6440. https://doi.org/10.1016/j.watres.2011.09.038.

[55] J. Xiao, S. Hao, Y. Qin, P. Qi, Z. Zhang, Y. Hu, Fouling-resistant reverse osmosis membranes grafted with 2-aminoethanethiol having a low interaction energy with charged foulants, NPJ Clean Water 7 (2024). https://doi.org/10.1038/s41545-024-00326-5.

[56] S.Z. Abdullah, P.R. Bérubé, D.J. Horne, SEM imaging of membranes: Importance of sample preparation and imaging parameters, J Memb Sci 463 (2014) 113–125. https://doi.org/10.1016/j.memsci.2014.03.048.

[57] K. Akhtar, S.A. Khan, S.B. Khan, A.M. Asiri, Scanning Electron Microscopy: Principle and Applications in Nanomaterials Characterization, in: Handbook of Materials Characterization, Springer International Publishing, Cham, 2018: pp. 113–145. https://doi.org/10.1007/978-3-319-92955-2_4.

[58] M. Abd Mutalib, M.A. Rahman, M.H.D. Othman, A.F. Ismail, J. Jaafar, Scanning Electron Microscopy (SEM) and Energy-Dispersive X-Ray (EDX) Spectroscopy, in: Membrane Characterization, Elsevier, 2017: pp. 161–179. https://doi.org/10.1016/B978-0-444-63776-5.00009-7.

[59] M.Z. Baykara, U.D. Schwarz, Atomic Force Microscopy: Methods and Applications, in: Encyclopedia of Spectroscopy and Spectrometry, Elsevier, 2017: pp. 70–75. https://doi.org/10.1016/B978-0-12-409547-2.12141-9.

[60] M. Wei, Y. Zhang, Y. Wang, X. Liu, X. Li, X. Zheng, Employing Atomic Force Microscopy (AFM) for Microscale Investigation of Interfaces and Interactions in Membrane Fouling Processes: New Perspectives and Prospects, Membranes (Basel) 14 (2024). https://doi.org/10.3390/membranes14020035.

[61] M. Chan, S. Ng, Effect of membrane properties on contact angle, in: AIP Conf Proc, American Institute of Physics Inc., 2018: p. 020035. https://doi.org/10.1063/1.5055437.

[62] M. Cheryan, Ultrafiltration and Microfiltration, Second Edi, CRC Press, 1998. https://doi.org/10.1016/j.bbrc.2004.06.056.

[63] H. Li, V. Chen, Membrane Fouling and Cleaning in Food and Bioprocessing, in: Membrane Technology, Elsevier, 2010: pp. 213–254. https://doi.org/10.1016/B978-1-85617-632-3.00010-0.

[64] G. Trägårdh, Membrane cleaning, Desalination 71 (1989) 325–335. https://doi.org/10.1016/0011-9164(89)85033-7.

[65] J.M. Arnal, B. Garcia-Fayos, M. Sancho, Membrane Cleaning, in: Expanding Issues in Desalination, InTech, 2011. https://doi.org/10.5772/19760.

[66] D.C. Montgomery, Design and analysis of experiments, 8th Edition, John Wiley & Sons, 2013.

[67] J. Antony, Fundamentals of Design of Experiments, in: Design of Experiments for Engineers and Scientists, Elsevier, 2003: pp. 6–16. https://doi.org/10.1016/B978-075064709-0/50003-X.

[68] B. Ait-Amir, P. Pougnet, A. El Hami, Meta-Model Development, in: Embedded Mechatronic Systems 2, Elsevier, 2015: pp. 151–179. https://doi.org/10.1016/B978-1-78548-014-0.50006-2.

[69] L.A. Sarabia, M.C. Ortiz, Response Surface Methodology, in: Comprehensive Chemometrics, Elsevier, 2009: pp. 345–390. https://doi.org/10.1016/B978-044452701-1.00083-1.

[70] K.-B. Park, C. Choi, H.-W. Yu, S.-R. Chae, I.S. Kim, Optimization of chemical cleaning for reverse osmosis membranes with organic fouling using statistical design tools, Environmental Engineering Research 23 (2018) 474–484. https://doi.org/10.4491/eer.2017.098.

[71] C. Wang, A. Wei, H. Wu, F. Qu, W. Chen, H. Liang, G. Li, Application of response surface methodology to the chemical cleaning process of ultrafiltration membrane, Chin J Chem Eng 24 (2016) 651–657. https://doi.org/10.1016/j.cjche.2016.01.002.

[72] S.S. Yoo, K.H. Chu, I.-H. Choi, J.S. Mang, K.B. Ko, Operating cost reduction of UF membrane filtration process for drinking water treatment attributed to chemical cleaning optimization, J Environ Manage 206 (2018) 1126–1134. https://doi.org/10.1016/j.jenvman.2017.02.072.

[73] E. de Jong, R.J.A. Gosselink, Lignocellulose-Based Chemical Products, Elsevier, 2014. https://doi.org/10.1016/B978-0-444-59561-4.00017-6.

[74] D. Fengel, G. Wegener, Chemical Composition and Analysis of Wood, in: Wood, de Gruyter, 1989: pp. 26–65.

[75] J. Gullichsen, Fiber line operations, in: J. Gullichsen, C.-J. Fogelholm (Eds.), Chemical Pulping, Fapet Oy, 1999: pp. 19–243.

[76] P. Niemz, C. Mai, U. Schmitt, Introduction to Wood Science, in: P. Niemz, A. Teischinger, D. Sandberg (Eds.), Springer Handbook of Wood Science and Technology, Springer, 2023: pp. 25–40. https://doi.org/10.1007/978-3-030-81315-4_2.

[77] E.P. Feofilova, I.S. Mysyakina, Lignin: Chemical structure, biodegradation, and practical application (a review), Appl Biochem Microbiol 52 (2016) 573–581. https://doi.org/10.1134/S0003683816060053.

[78] G. Gellerstedt, G. Henriksson, Lignins: Major Sources, Structure and Properties, in: Monomers, Polymers and Composites from Renewable Resources, Elsevier, 2008: pp. 201–224. https://doi.org/10.1016/B978-0-08-045316-3.00009-0.

[79] E. Sjöström, Wood Pulping, in: Wood Chemistry, 1993: pp. 114–164. https://doi.org/10.1016/b978-0-08-092589-9.50011-5.

[80] H. Tran, E.K. Vakkilainen, The Kraft Chemical Recovery Process, TAPPI Kraft Recovery Course (2012) 1–8.

[81] T.M. Grace, E.W. Malcolm, eds., Pulp and Paper Manufacture Vol. 5 Alkaline Pulping, 3rd edition, Technical Section Canadian Pulp and Paper Association, 1989.

[82] H. Loufti, B. Blackwell, V. Uloth, Lignin recovery from kraft black liquor: preliminary process design, Tappi J 74 (1991) 203–210.

[83] G. Gellerstedt, P. Tomani, P. Axegård, B. Backlund, Lignin Recovery and Lignin-Based Products, in: Integrated Forest Biorefineries, The Royal Society of Chemistry, 2012: pp. 180–210. https://doi.org/10.1039/9781849735063-00180.

[84] E. Välimäki, P. Niemi, K. Haaga, A Case Study on the Effects of Lignin Recovery on Recovery Boiler Operation, in: 2010. https://doi.org/10.13140/2.1.1777.5046.

[85] T. Li, S. Takkellapati, The current and emerging sources of technical lignins and their applications, Biofuels, Bioproducts and Biorefining 12 (2018) 756–787. https://doi.org/10.1002/bbb.1913.

[86] A. Berlin, M. Balakshin, Industrial Lignins, in: Bioenergy Research: Advances and Applications, Elsevier, 2014: pp. 315–336. https://doi.org/10.1016/B978-0-444-59561-4.00018-8.

[87] A.-S. Jönsson, Membranes for lignin and hemicellulose recovery in pulp mills, in: Membrane Technologies for Biorefining, Elsevier, 2016: pp. 105–133. https://doi.org/10.1016/B978-0-08-100451-7.00005-0.

[88] E.K. Pye, Industrial Lignin Production and Applications, 2008. https://doi.org/10.1002/9783527619849.ch22.

[89] P. Tomani, The LignoBoost Process, Cellulose Chemistry and Technology 44 (2010) 53–58.

[90] Valmet, LignoBoost® - lignin from pulp mill black liquor, (2021). https://www.valmet.com/pulp/other-value-adding-processes/lignin-extraction/ (accessed December 15, 2021).

[91] O. Wallberg, A.-S. Jönsson, Separation of lignin in kraft cooking liquor from a continuous digester by ultrafiltration at temperatures above 100°C, Desalination 195 (2006) 187–200. https://doi.org/10.1016/j.desal.2005.11.011.

[92] M. Mänttäri, A. Pihlajamäki, E. Kaipainen, M. Nyström, Effect of temperature and membrane pre-treatment by pressure on the filtration properties of nanofiltration membranes, Desalination 145 (2002) 81–86. https://doi.org/10.1016/S0011-9164(02)00390-9.

[93] W.X. Yao, K.J. Kennedy, C.M. Tam, J.D. Hazlett, Pre-treatment of kraft pulp bleach plant effluent by selected ultrafiltration membranes, Can J Chem Eng 72 (1994) 991–999. https://doi.org/10.1002/cjce.5450720608.

[94] M. Mänttäri, J. Nuortila-Jokinen, M. Nyström, Evaluation of nanofiltration membranes for filtration of paper mill total effluent, Filtration & Separation 34 (1997) 275–280. https://doi.org/10.1016/S0015-1882(97)84794-5.

[95] A. Al-Amoudi, R.W. Lovitt, Fouling strategies and the cleaning system of NF membranes and factors affecting cleaning efficiency, J Memb Sci 303 (2007) 4–28. https://doi.org/10.1016/j.memsci.2007.06.002.

[96] T. Mohammadi, S.S. Madaeni, M.K. Moghadam, Investigation of membrane fouling, Desalination 153 (2003) 155–160. https://doi.org/10.1016/S0011-9164(02)01118-9.

[97] G. Rudolph, A. Hermansson, A.-S. Jönsson, F. Lipnizki, In situ real-time investigations on adsorptive membrane fouling by thermomechanical pulping process water with quartz crystal microbalance with dissipation monitoring (QCM-D), Sep Purif Technol 254 (2021) 117578. https://doi.org/10.1016/j.seppur.2020.117578.

[98] M. Bartlett, M.R. Bird, J.A. Howell, An experimental study for the development of a qualitative membrane cleaning model, J Memb Sci 105 (1995) 147–157. https://doi.org/10.1016/0376-7388(95)00052-E.

[99] L. Delin, N. Berglin, Å. Samuelsson, A. Lundström, B. Backlund, Å. Sivard, FRAM Final report-Application area: Model mills and system analysis, Stockholm, Sweden: STFI-Packforsk (2005).

[100] M. Bagheri, A. Akbari, S.A. Mirbagheri, Advanced control of membrane fouling in filtration systems using artificial intelligence and machine learning techniques: A critical review, Process Safety and Environmental Protection 123 (2019) 229–252. https://doi.org/10.1016/j.psep.2019.01.013.

[101] P. Dansawad, Y. Li, Y. Li, J. Zhang, S. You, W. Li, S. Yi, Machine learning toward improving the performance of membrane-based wastewater treatment: A review, Advanced Membranes 3 (2023). https://doi.org/10.1016/j.advmem.2023.100072.

Printed by Media-Tryck, Lund 2024 NORDIC SWAN ECOLABEL 3041 0903

ISBN: 978-91-8096-062-5

Department of Process and
Life Science Engineering
Faculty of Engineering
Lund University